arXiv:1610.00039v1 [stat.AP] 30 Sep 2016

Leveraging Contact Network Information in Clustered Randomized Trials of Infectious Processes

Patrick Staples*[1], Mélanie Prague†[1], De Gruttola Victor‡[1], and Jukka-Pekka Onnela§[1]

[1]Department of Biostatistics, Harvard University, Boston, MA 02115, USA

Abstract

In some infectious processes, transmission occurs between specific ties between individuals, which ties constitute a contact network. To estimate the effect of an exposure on infectious outcomes within a collection of contact networks, the analysis must adjust for the correlation of outcomes within networks as well as the probability of exposure. This estimation process may be more statistically efficient when leveraging baseline covariates related to both the exposure and infectious outcome. We investigate the extent to which gains in statistical efficiency depend on contact network structure and properties of the infectious process. To do this, we simulate a stochastic compartmental infection on a collection of contact networks, and employ the observational augmented GEE using a variety of contact network and baseline infection summaries as adjustment covariates. We apply this approach to estimate the effect of leadership and a concurrent self-help program in the spread of a novel microfinance program in a collection of villages in Karnataka, India.

*email: patrickstaples@fas.harvard.edu
†email: mprague@hsph.harvard.edu
‡email: degrut@hsph.harvard.edu
§email: onnela@hsph.harvard.edu

1 Introduction

Infectious processes spread through specific contact ties between individuals. For any fixed time, these transmission routes constitute a network[1 2 3 4 5]. For a deleterious infection, a treatment aims to reduce the probability of transmission from one node to another. For example, in the context of HIV, one strategy to reduce the overall rate of transmission is to test and treat all infected individuals, which is the goal of several ongoing clinical trials[6 7 8]. Other spreading processes propagate through specific ties between individuals, such as diffusive processes of ideas or practices[9], and can also be modeled as an infectious process.

To determine if a treatment is effective, one might randomly assign some individuals to receive the treatment, and others to receive standard care or a placebo, which randomization ensures balance on average in the predictors between the two arms. This type of experiment is called a *Randomized Controlled Trial* (RCT). When this is not possible, a population of individuals may be available for observation in which two or more groups have different exposures related to the outcome, which can be made to resemble an RCT if all confounders are correctly adjusted for[10 11]. In addition, *interference* occurs when an individual's outcome depends on the outcomes of other individuals in addition to exposure[12]. This can be avoided by assuming that clusters of individuals are independent, and adjusting for the correlation of outcomes within clusters[13 14] as well as the probability of exposure[10]. Dependent outcomes within clusters generally results in a decrease in statistical *power*, or the probability of detecting an exposure effect if one exists, and this decrease can depend on epidemic dynamics as well as within-cluster network structure[15].

Generalized Estimating Equations (GEEs)[16] are a semi-parametric approach for estimating a treatment effect in randomized trials when outcome data are correlated within clusters[13]. This approach produces unbiased estimates of the average marginal treatment effect across all clusters, whereas mixed effect models provide an estimated intervention effect conditional on adjustment covariates[17]. Accounting for the correlation between baseline covariates and the outcome can improve the efficiency of treatment effect estimates, using either the augmented GEE[18] or other semiparametric approaches, such as targeted maximum likelihood estimation (TMLE)[19]. When the exposure is not randomized, estimating the effect of exposure without bias requires that the propensity that each cluster is exposed to treatment be correctly estimated. Few studies of infectious processes so far use contact network information to improve statistical efficiency using these approaches[8].

This paper investigates the degree to which exposure effect estimates in simulated and empirical observational studies of epidemic processes are improved by adjusting for features of the contact networks and infections at baseline. Section 2 gives details on the network generation framework, infectious process, and the estimation procedures used to evaluate the effect of exposure while adjusting for network features. Section 3 details a series of simulations of observational studies using this framework. Section 4 applies this approach to an empirical dataset, treating the spread of a novel microfinance program as an

infectious process in a collection of villages in Karnataka, India. Section 5 provides concluding remarks.

2 Methods

Contact Network Structure

A simple network $\mathcal{G}$ consists of set of nodes $\mathcal{N} = \{1, ..., n\}$ and edges $\mathcal{E} \subseteq \mathcal{N} \times \mathcal{N}$. The edges may be described in an *adjacency matrix* $\mathbf{E}_{n \times n}$, where element $\mathbf{E}_{jj'} = \mathbf{E}_{j'j}$ has value 1 if an edge exists between nodes j and j', and a 0 otherwise. One specific network model, the stochastic blockmodel[20], assumes that each node j belongs to only one block b_j in a partition of nodes $\mathcal{B} = \{1, ..., B\}$. The complete set of node memberships may be represented compactly as a vector $\mathbf{b} = \{b_1, ..., b_n\}$. In this model, the probability of there being an edge between two nodes j and j' depends only on their block membership $P(\mathbf{E}_{jj'} = 1) = p_{b_j b_{j'}}$. Karrer and Newman[1] extend this model to the *Degree-Corrected Stochastic Blockmodel*, in which each node j has arbitrary expected degree $\theta_j := \mathbb{E}(k_j)$, where k_j is the observed *degree* $\sum_{j'} \mathbf{E}_{jj'}$ for node j. The likelihood of this model assumes that the mean number of edges $\nu_{jj'}$ between any two nodes j and j' is the product of the expected degree of nodes j and j' (θ_j and $\theta_{j'}$, respectively), multiplied by the expected amount of mixing $\omega_{b_j, b_{j'}}$ between the blocks to which j and j' belong. The full likelihood of this model is:

$$P(\mathbf{E}|\theta, \omega, \mathbf{b}) = \prod_{j<j'} \frac{\nu_{jj'}^{\mathbf{E}_{jj'}}}{\mathbf{E}_{jj'}!} \exp(-\nu_{jj'}) \times \prod_{j} \frac{\left(\frac{1}{2}\nu_{jj}\right)^{\mathbf{E}_{jj'}/2}}{(\mathbf{E}_{jj'}/2)!} \exp\left(-\frac{1}{2}\nu_{jj}\right) \tag{1}$$

$$\nu_{jj'} = \theta_j \theta_{j'} \omega_{b_j, b_{j'}} \tag{2}$$

Equation 1 assumes $b_{jj'}$ is Poisson distributed (allowing for multiple edges between pairs of nodes), which converges to a simple Bernoulli network for sparse networks in the limit $n_i \to \infty$[1]. The second half of the likelihood contains factors of one half to account for the fact that *self-edges* (edges from one node to itself) are counted twice by this indexing.

In addition to block structure and node degree, networks may vary in the extent to which degrees of adjacent nodes are correlated[22]. One metric for summarizing this property is *degree assortativity*, which is the Pearson correlation coefficient of degrees of adjacent nodes taken over all network edges[23]. Degree assortativity can be varied by performing *degree assortative rewiring*, which increases or decreases the assortativity in the network while preserving block structure and each node's degree[24 25]. This is performed by randomly selecting two edges within a block pair and rewiring them, as described in Algorithm 1. A diagram of this process is shown in Figure 1. To decrease assortativity, the inequality in Step 3 must be reversed.

Algorithm 1: Edge Rewiring to Adjust Assortativity

1 Select two blocks b_l and $b_{l'}$ at random.

2 Select two edges (N_1, N_2) and (N_3, N_4) at random between blocks b_l and $b_{l'}$.

3 If $|k_{N_1} - k_{N_2}| + |k_{N_3} - k_{N_4}| > |k_{N_1} - k_{N_4}| + |k_{N_2} - k_{N_3}|$:

Remove edges (N_1, N_2) and (N_3, N_4)

Add edges (N_1, N_4) and (N_2, N_3)

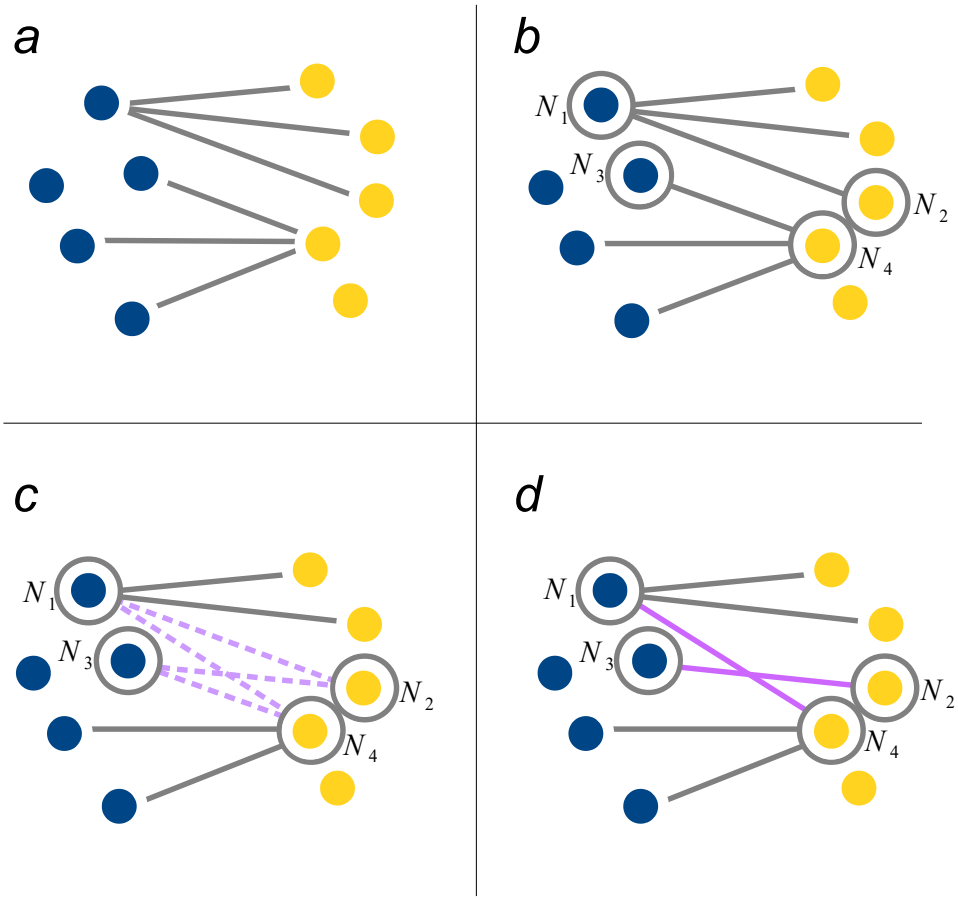

Figure 1: A schematic of degree assortative rewiring. Panel **a** displays a network, containing nodes $N_1, ..., N_4$. Panel **b** highlights two edges selected within the same block pair. Panel **c** shows a potential rewiring, which will only occur if rewiring will increase assortativity. In this case, rewiring would increase degree assortativity, and panel **d** displays the rewiring.

Infectious Process

An infectious process on the collection of networks[26] is simulated by employing a stochastic compartmental *SI* model[27], shown in Algorithm 2. $S\%$ of all nodes are initially selected to be infected at random across all study networks $i = 1, ..., m$. Then, infected node j in network cluster i selects $q_{i;j}$ of their $k_{i;j}$ neighbors and infect them with probability p_0, where $q_{i;j}$ is the node's *infectivity* (described in more detail below). This process is repeated until $B\%$ of the population is infected at baseline. Half of the clusters are determined to be exposed ($A_i = 1$) or unexposed ($A_i = 0$), and the infectious process continues for T time steps with a probability to infect p_0 for unexposed clusters, and p_1 for exposed clusters.

Algorithm 2: Stochastic Compartmental Epidemic Process

1 $S\%$ of all nodes are selected uniformly at random to be initially infected.

2 Until $B\%$ population incidence:

  For each infected node j (in random order):

  a Successively select $q_{i;j}$ neighbors.

  b If neighbor j' is already infected, do nothing. If not, infect with probability p_0.

3 Repeat T times:

  For each infected node j (in random order):

  a Successively select $q_{i;j}$ neighbors.

  b If neighbor j' is already infected, do nothing. If not, infect with probability:

  p_0 for those in unexposed clusters,

  p_1 for those in exposed clusters.

In this process, infectivity $q_{i;j}$ is the number of individuals node j may infect at a given time, which may vary between 0 and $k_{i;j}$. Zhou et al.[28] showed that the properties of network spread can depend strongly on infectivity. Unit infectivity and degree infectivity occur when an individual attempts to infect either one partner (selected at random) or all partners, respectively. Illustrative diagrams of the infectious process over time are given in the Supplementary Section `S1`.

Summaries of Network Structure and Infectious Process

While a network i consists of pairwise connections between individuals j and j', properties of the network can be summarized for each node $\mathbf{X}_{i;j}$. This vector is composed of a small number of functions of the network to which the nodes belong, which can be used for the estimation of the effects of exposure, discussed in the following section. Some of these are constant per network, and some are different for every individual. They fall into four broad classes: those involving degree, mesoscopic structure (structure with a size between that of the node and entire network), baseline infections, and combinations of these.

Let $\mathbf{E}_i$ represent the $n_i \times n_i$ adjacency matrix for the network structure in cluster i. One network summary for each node j is its degree, $k_{i;j} = \sum_{j'} \mathbf{E}_{i;jj'}$. Mean neighbor degree $\sum_{j'} \frac{\mathbf{E}_{i;jj'} k_{i;j'}}{k_{i;j}}$ is the unweighted average of a node's neighbors' degrees. *Assortativity* is a composite measure of mean neighbor degree across the entire network, defined previously.

Network features may also capture *mesoscopic* network structure, or structure existing between local and global scales of the network. For example, two blocks of nodes ($b_{i;j} \in \{1, 5\}$) may be more highly connected to all other blocks the simulated networks. Another mesoscopic structure is a *connected component*, or subset of nodes for which a path exists between each pair of nodes. A *path* exists between two node j and j' if and only if there exists a subset of edges $\mathcal{E}_{i;jj'} \subseteq \mathcal{E}_i$ in the network that connect nodes j and j'. The components of the network $c \in 1, ..., C_i$ are assumed to be ordered from largest to smallest. The largest component in the network contains $\sum_j \mathbb{I}(c_{i;j} = 1)$ nodes. The mean component size is n_i/C_i, the number of components C_i, and the size of the component each node belongs to is $\sum_{j'} \mathbb{I}(c_{i;j} = c_{i;j'})$.

Another summary feature is the infectious status of each node in the network at baseline. One simple metric is the number of infected neighbors at baseline for each node $\sum_{j'} \mathbf{E}_{i;jj'} I_{i;j'}(0)$, or the number of infected individuals belonging to the same component as a given node $\sum_{j'} \mathbb{I}(c_{i;j} = c_{i;j'}) I_{i;j'}(0)$. Another metric is the length of the shortest path between each node j and each infected individual j' at baseline. The shortest path length between nodes j and j' is $d_{i;jj'}$, where $d_{i;jj'} := \infty$ when no path exists between the two nodes. The shortest path length from the closest node infected at baseline is $\min_{j'} d_{i;jj'}$, with inverse $(\min_{j'} d_{i;jj'})^{-1}$. The sum of the inverse path lengths to node j is $\sum_{j'} (d_{i;jj'})^{-1}$. While these final metrics would be difficult to determine with limited knowledge about a network, we examine whether their inclusion in the analysis yields strong enough improvements to warrant the efforts to gather the required network data. Additional metrics may also be defined for multilayer networks, in which several edges with distinct labels may be shared between nodes[35]. The outcome model may incorporate any subset of covariates, for example as obtained from a stepwise selection procedure[34]. Table 1 summarizes these network features.

None: No adjustment term	
$X^{(1)}$: Degree	$k_{i;j}$
$X^{(2)}$: Mean neighbor degree	$\sum_{j'} \frac{A_{i;jj'}k_{i;j}}{k_{i;j}}$
$X^{(3)}$: Assortativity	$\underset{(j,j')\in\mathcal{E}_i}{\text{cor}}\, k_{i;j}, k_{i;j'}$
$X^{(4)}$: Member of connected block	$\mathbb{I}(b_{i;j} \in \{1, 5\})$
$X^{(5)}$: Size of largest component	$\sum_j \mathbb{I}(c_{i;j} = 1)$
$X^{(6)}$: Mean component size	n_i/C_i
$X^{(7)}$: Number of components	C_i
$X^{(8)}$: Size of node's component	$\sum_{j'} \mathbb{I}(c_{i;j} = c_{i;j'})$
$X^{(9)}$: Total neighbor infections at baseline	$\sum_{j'} \mathbf{E}_{i;jj'} I_{i;j'}(0)$
$X^{(10)}$: Total code's component infections at baseline	$\sum_{j'} \mathbb{I}(c_{i;j} = c_{i;j'}) I_{i;j'}(0)$
$X^{(11)}$: 1/nearest infected path length at baseline	$(\min_{j'} d_{i;jj'})^{-1}$
$X^{(12)}$: $\sum_{j'}$ 1/path length to infected j at baseline	$\sum_{j'} (d_{i;jj'})^{-1}$
$X^{(13)}$: Linear combination of all the above	
$X^{(14)}$: Linear combination of a selection of the above	

Table 1: A collection of summaries of the contact network and infections at baseline.

Estimation of the Effect of the Exposure

Consider an observational study that consists of $i = 1, ..., m$ clusters with $j = 1, ..., n_i$ individuals per cluster, and $\sum_i n_i = N$ total individuals in the study. For each individual, the outcome for individual j in cluster i ($Y_{i;j}$) is 1 if the individual is infected by the end of the study, and 0 otherwise. The vector $\mathbf{Y}_i = (Y_{i;1}, ..., Y_{i;n_i})^\top$ is the associated vector of outcomes in cluster i. Each individual belongs to a cluster specific contact network with corresponding adjacency matrix $\mathbf{E}_i$. We assume there is no mixing across clusters, *i.e.*, clusters are independent. In addition, each individual has a set of P cluster-level and individual-level covariates $\mathbf{X}_{i;j} = (X^{(1)}_{i;j}, ..., X^{(P)}_{i;j})^\top$, with all covariates represented compactly as $\mathbf{X}_i = (\mathbf{X}_{i;1}, ..., \mathbf{X}_{i;n_i})^\top$. Each cluster is either unexposed ($A_i = 0$), or exposed ($A_i = 1$). The causal parameter of interest β_A is the average risk difference between outcomes, comparing exposed to unexposed clusters. This quantity is estimated in the marginal regression model $\mathbb{E}(Y_{i;j}|A_i) = \mu_i(\beta, A_i) = \beta_0 + \beta_A A_i$. Because the true data generating mechanism is a stochastic epidemic process on a collection of networks, the true effect of an exposure is not directly specified, and can only be determined through extensive simulation[29]. The GEE-based approach, reweighted for inverse probability of exposure, gives estimates that are consistent and asymptotically normal[30], so β_A is defined as the average of the $\widehat{\beta}_A$ estimates over R stochastic replicates.

By adjusting for chance imbalance in exposure groups and accounting for correlation between covariates and the outcome, it is possible to improve the efficiency of estimation by incorporating baseline covariates $\mathbf{X}_i$ in the approach. This consists of using an inverse probability weighted GEE, including a propensity score to estimate the probability of exposure assignment[31]. Using the augmented GEE approach for observational data,[32] the exposure effect is the vector of coefficients $\boldsymbol{\beta}$ that solves the

following estimating equation:

$$0 = \sum_{i=1}^{m} \Bigg[\mathbf{D}_i^T \mathbf{V}_i^{-1} \mathbf{G}_i(\mathbf{X}_i, A_i, \eta_G) \left(\mathbf{Y}_i - \mathbf{B}_i(\mathbf{X}_i, A_i, \eta_B) \right) \sum_{a=0,1} \mathbf{D}_i^T(a) \mathbf{V}_i^{-1}(a) \Big(\mathbf{B}_i(\mathbf{X}_i, A_i = a, \eta_B) - \mu_i(\boldsymbol{\beta}, A_i = a) \Big) \Bigg], \quad (3)$$

where $\mathbf{D}_i = \frac{\partial \mu_i(\boldsymbol{\beta}, A_i)}{\partial \boldsymbol{\beta}^T}$ is the design matrix. The covariance matrix $\mathbf{V}_i$ is equal to $\phi \mathbf{U}_i^{1/2} \mathbf{C}(\alpha) \mathbf{U}_i^{1/2}$, where $\mathbf{U}_i$ a diagonal matrix with elements $\text{var}(Y_{i;j})$, ϕ is the dispersion parameter, and $\mathbf{C}(\alpha)$ is the working correlation structure with non-diagonal terms α. The $n_i \times n_i$ matrix $\mathbf{G}_i(\mathbf{X}_i, A_i, \eta_G) = \text{diag} \left[\frac{A_i}{g_i(\mathbf{X}_i^C, \eta_G)} + \frac{1-A_i}{1-g_i(\mathbf{X}_i^C, \eta_G)} \right]_{j=1,\ldots,n_i}$ is the inverse probability weighting for each cluster, where $g_i(\mathbf{X}_i^C, \eta_G)$ is the *Propensity Score* (PS) of exposure assignment for cluster i. The PS is correctly specified if it equals the true exposure assignment mechanism $g_i(\mathbf{X}_i^C, \eta_G) = \mathbb{P}(A_i = 1 | \mathbf{X}_i)$, where η_G are nuisance parameters to be estimated. The PS is obtained by fitting a binary response model that regresses the exposure indicator A_i on cluster-level covariates and mean individual-level covariates aggregated at the cluster level $\mathbf{X}_i^C = \frac{1}{n_i} \sum_{j=1}^{n_i} \mathbf{X}_{i;j}$. The *Outcome Model* (OM) $\mathbf{B}_i(\mathbf{X}_i, A_i = a, \eta_B) = \text{diag}[B_{i;j}(\mathbf{X}_i, A_i = a, \eta_B)]_{j=1,\ldots,n_i}$ is an arbitrary function of $\mathbf{X}_i$ given for each intervention group, where η_B are nuisance parameters to be estimated. The variance of $\boldsymbol{\beta}$ is estimated by using a sandwich estimator. The estimator is most efficient if $B_{i;j}(\mathbf{X}_i, A_i = a, \eta_B) = \mathbb{E}(Y_{i;j} | \mathbf{X}_i, A_i = a)$. The model for the OM can be selected with a data-driven approach (such as stepwise) without loss of consistency[33]. This approach estimates the true exposure effect without bias if the PS is correctly specified[32].

3 Simulation

Specification of Simulation Scenarios

This section specifies the network block structure and epidemic spread used in the simulation of observational studies. In anticipation of the empirical dataset to follow, each simulated study consists of an infectious process propagating on $m = 48$ clusters (networks) of sizes ranging from $n = 120$ to 280, with an average size of size 200, totaling 9600 individuals. For $R = 1000$ simulation replicates each, six binary aspects are varied combinatorially to create 2^6 scenarios, with details to follow:

$\mathbf{a_1}$: Mean degree of each node	$\{2, 10\}$
$\mathbf{a_2}$: Node degree distribution	$\in \{\text{Poisson}, \text{Powerlaw}\}$
$\mathbf{a_3}$: Assortativity	$\{-0.3, 0.3\}$
$\mathbf{a_4}$: Mixing structure	$\{\text{Random}, \text{Heterogeneous}\}$
$\mathbf{a_5}$: Infectivity	$\{\text{Unit}, \text{Degree}\}$
$\mathbf{a_6}$: Seed and Baseline Prevalence	$(S, B) \in \{(1, 2)\%, (10, 25)\%\}$

Table 2: A summary of the simulation aspects investigated, for which each combination is evaluated.

Block Structure

Two types of block structure are considered here, both of which are special cases of *bipartite* networks. A bipartite network is one in which each node belongs to exactly one of two groups, and edges only exist between members of different groups. Each network in our simulation comprises eight blocks: four blocks in male and female groups, assuming a heterosexual (bipartite) contact network. Two different block structures are considered: random, and heterogeneous. For a complete description of the block structures used, see Supplementary Section `S2`. A diagram of these structures is shown in Figure 2.

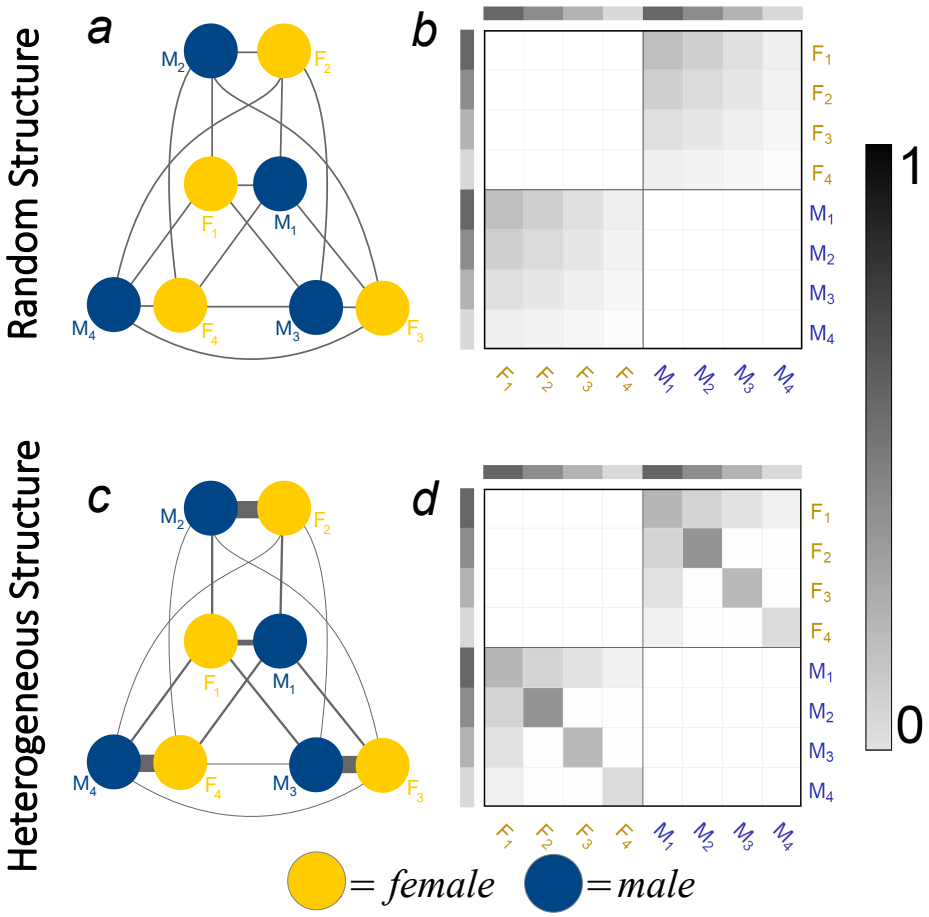

Figure 2: The top and bottom rows show the two kinds of mixing used, and the left and right panels show the block mixing structure and block mixing matrices, respectively. In all diagrams, the eight blocks represent the eight groups of nodes, four female ($F_1, ..., F_4$ in yellow) and four male ($M_1, ..., M_4$ in blue), that partition each network. Both of these block structures are bipartite, meaning edges only exist between nodes in Blocks F_l and $M_{l'}$. Panel **a** shows the random block structure, with lines connecting blocks that share edges. Panel **b** shows the corresponding mixing matrix, where the rows and columns represent each block, and shade color represents the fraction of edges shared between members of each block. The shaded bar shows the shade corresponding to the number edges belonging between group pairs as a fraction of the total number of edges. Panels **c** and **d** show the block mixing structure and matrices for the heterogeneous structure, respectively.

Epidemic Process

The epidemic process is assumed to continue for $T = 5$ times steps. For simplicity, we assume a strong exposure effect; for exposed and unexposed clusters, the probability each infected node infects a selected neighbor is $p_1 = 0.1$ and $p_0 = 0.3$, respectively.

Probability of Cluster Exposure

The probability that a given cluster is exposed is a simple logistic function of a single cluster level covariate, *i.e.*, the number of infected neighbors at baseline summed for all nodes in each cluster (see Equation 4). For each scenario, ψ_0 and ψ_A are selected such that this probability is between $(10, 90)\%$ for all clusters. In the estimation process, the simple regression used for the exposure propensity model includes this covariate, ensuring asymptotically unbiased estimation of the exposure effect.

$$\mathbb{P}(A_i = 1|\mathbf{X}_i) = \text{expit}\left(\psi_0 + \psi_A \sum_j X_{i;j}^{(9)}\right) \tag{4}$$

$$= \text{expit}\left(\psi_0 + \psi_A \sum_j \sum_{j'} \mathbf{E}_{i;jj} I_{i;j'}(0)\right) \tag{5}$$

Performance Metrics

For $r = 1, ..., R$ replicates, the augmented GEE estimates of exposure effect size $\widehat{\beta}_r$ and estimate standard deviation $\widehat{\text{sd}}_r(\widehat{\beta}_r)$ are evaluated. Because the probability of cluster-level exposure is correctly specified, the estimated exposure estimate for each simulation $\widehat{\beta}_r$ is unbiased. Therefore, the true exposure effect across all simulations is estimated as the average of all exposure effect estimates, $\beta_A := \frac{1}{R}\sum_{r=1}^{R} \widehat{\beta}_r$.

The metric for the gained improvement associated with the augmentation term is the percent reduction in root mean squared error (RMSE) for each adjustment covariate set, comparing the augmentation adjustment $\widehat{\text{RMSE}}_{\text{adj}}$ to that of the unadjusted GEE ($\widehat{\text{RMSE}}_{\text{GEE}}$):

$$\widehat{\text{Improvement}} := 100 \times \left(1 - \frac{\widehat{\text{RMSE}}_{\text{adj}}}{\widehat{\text{RMSE}}_{\text{GEE}}}\right) \tag{6}$$

Simulation Results

Adjusting for covariates increases efficiency when the covariate is related to outcomes as well as the exposure. In the simulated studies, the adjustment covariates are correlated with both the outcome and exposure, with full results given in Supplementary Section S3. We therefore expect reductions in the RMSE upon employing a combination of them in the outcome model. Because the process includes a novel infection spreading of moderate duration spreading only through network ties, we predict that adjusting for each node's number of infected neighbors at baseline (covariate $X^{(9)}$ in Table 1) to be a significant adjustment covariate. We also investigate more data-adaptive approaches, such as including all covariates in Table 1 as well as a stepwise selection procedure. Table 3 reports empirical bias, estimated and empirical variance of the exposure effect estimate, improvement in RMSE, statistical power, and coverage averaged across of the 2^6 observational scenarios (with standard deviations across scenarios in parentheses).

	None	Only $X^{(9)}$	All	Step
Bias	0	-0.0232	-0.0329	-0.0319
Standard Error	1.68	0.84	0.6	0.6
Empirical SE	1.39	0.7	0.64	0.63
Improvement	0(0)	43(23)	42(31)	43(30)
Power	48.1	90.9	94.3	94.2
Coverage	98(2)	97(2)	92(4)	92(4)

Table 3: Exposure effect statistics averaged across each simulation aspect. Each row displays a metric, and each column displays an adjustment feature or strategy. Standard deviations across scenarios are shown in parentheses.

Across most all scenarios, covariate adjustment leads to significant gains in power. In addition, coverage is adequate for many scenarios, ensuring a valid interpretation of power for those scenarios. This indicates low bias, albeit moderately anti-conservative estimates of standard error. However, coverage can be low when using all covariates or a stepwise selection of them; this lower coverage can be caused by overfitting in the outcome model.

Covariate Selection

The distribution of the proportion of occasions each covariate is selected by stepwise selection (minimizing AIC) for inclusion in the outcome model is evaluated for each scenario, given in Figure 3. This figure shows that some covariates are very frequently selected for inclusion, including degree (covariate $X^{(1)}$) and covariates related to infection at baseline (covariates $X^{(9)} - X^{(12)}$), whereas others are selected in a range of frequencies. The outcomes models for the two exposure groups share broad similarity.

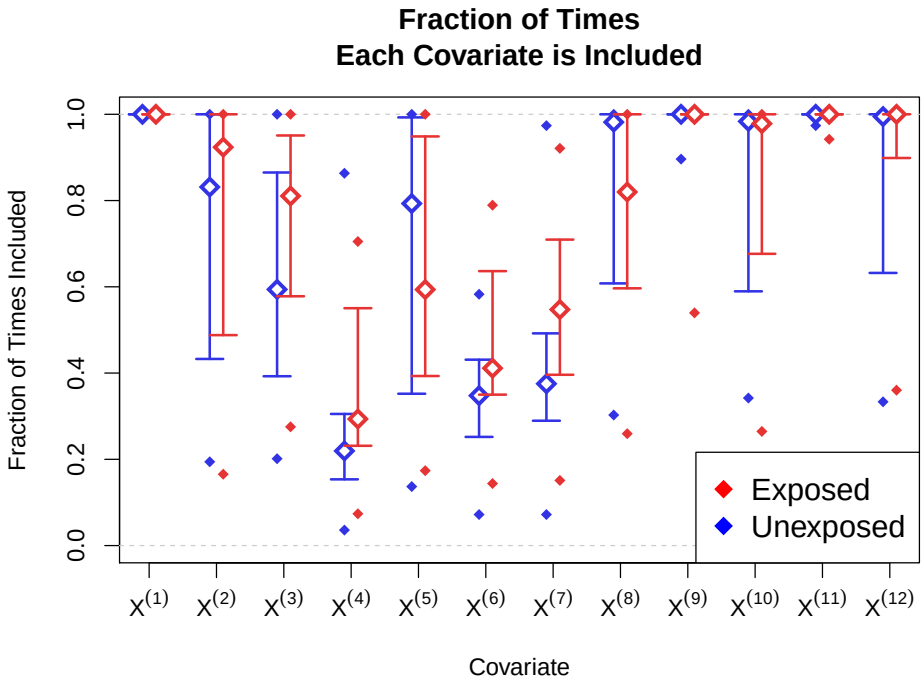

Figure 3: The distribution of the proportion of occasions each covariate is included. The covariates along x axis are described in Table 1. Blue bars show results for the exposed group, and red bars show results for the unexposed group. The middle values represent medians, the bars represent the (25, 75)% quartiles across each scenario, and endpoints indicate minima and maxima.

Result Modifications by Scenario

Assumptions about the simulated infectious process affect study metric such as bias and improvement in RMSE. The size of these effects are evaluated using simple linear regression, treating each statistic as the outcome, and binary aspects of the simulation as Bernoulli covariates. The coefficients resulting from this model represent the percent improvement resulting from changing one aspect from 0 to 1, holding all other simulation aspects constant. The percent improvement in RMSE is shown in Table 4; related metrics are available in the Supplementary Section S3. To provide guidance on how to interpret coefficients, we provide an example of a description of a coefficient of improvement modification by singling out the row "Degree Infectivity" and column $X^{(9)}$. Holding constant average degree, degree distribution, network assortativity, community structure, and infectivity, an epidemic process exhibiting high baseline prevalence shows an additional improvement of 27 percentage points in RMSE compared to an epidemic process exhibiting unit infectivity. Therefore, using adjustment variable $X^{(9)}$ (total number of infected neighbors at baseline) is more important if the observation of the epidemic begins with a high baseline compared to a low baseline. This suggests that a node's local network of partners and their infectious status can be quite predictive of the risk acquire the infection, a finding that has also been reported by Ghani et al.[36]

	Only $X^{(9)}$	All	Step
(Intercept)	41	15	18
High vs. Low Degree	-13	-2	-3
Powerlaw vs. Poisson	-16	1	-0
Assortative vs. Disassortative	5	8	7
Communities vs. No Communities	1	5	5
Degree vs. Unit Infectivity	1	-0	-1
High vs. Low Baseline	27	44	42

Table 4: Percent estimate improvement modification in RMSE modified by each simulation aspect. Each row displays an aspect, and each column displays an adjustment feature or strategy.

An analysis of which features are selected in the stepwise procedure for each simulation scenario is given in Supplementary Section S4. While we have considered a range of simulation variants, the modeling assumptions may not hold in an empirical spreading process, such as the process being well-characterized by an SI process propagating on a fixed network.

4 Application to Empirical Data

This section describes an application of our approach to incorporating contact network information in the estimation of exposure effects in the adoption of microfinance loans in a collection of 49,707 individuals in 49 villages in Karnataka, India[37]. The adoption of the loan program is an example of a diffusive process[9]. However, because the microfinance program was novel to the region (designed to be spread by word-of-mouth through community leaders) and its impact was assessed for a fixed time, we assume the diffusion process spreads can also be described as an infectious process. Six months before their introduction, leaders from each village (14.7% of the total population) were selected to attend an informational meeting about the program, and asked to inform others about it. Sociodemographic information (such as age and sex) were gathered for some individuals (totalling 12,122) in each village, as well as which households individuals belong to. Households were also offered the opportunity to concurrently enroll in a self-help program. In addition, the networks of each village were assessed, where edges in each network are social, familial, or economic ties. The outcome for each individual is whether they belong to a household that eventually participated in the microfinance program.

Most Similar Simulation Scenario

The participant network in this data exhibits a high degree ($\overline{k} = 16.0$, averaged across all participating villages). Additionally, the empirical degree distribution for this dataset does not have a fat tail, with details in the Supplementary Section S5.

The contacts networks exhibit a mean degree assortativity of 0.346. Individuals belong to households, implying community structure, and leaders were encouraged to inform all individuals they know, suggesting degree infectivity. Finally, individuals who were leaders as well as took up microfinance total 3.1%, indicating a low exposure at baseline. In combination, these aspects are most similar to the simulation scenario shown in Table 5, which shows key statistics for this configuration. This configuration exhibits good statistical coverage and high improvement in the RMSE for each adjustment strategy.

	None	Only $X^{(9)}$	All	Step
Bias	0.00	0.10	0.10	0.10
SE	1.80	1.10	0.80	0.80
Empirical SE	2.10	1.60	1.00	1.00
Improvement	0.00	25.52	52.27	52.46
Power	99	99	100	100
Coverage	98	96	95	96

Table 5: The assortment of statistics for the simulation scenario most similar to the Karnataka dataset.

Analysis Results

We define two exposures related to different proportions of microfinance uptake for each village. Exposure 1 defines a village as exposed if the fraction of households in the village containing leaders is in the top quartile comparing across all villages. This corresponds to the hypothesis that villages containing more leaders than other villages has a higher or lower rate of microfinance uptake. Exposure 2 is defined as whether the fraction of individuals in the village participating in the concurrent self-help program was greater than the top quartile. This corresponds to the hypothesis that villages containing more individuals willing to participate in other programs are also willing to participate in the new microfinance program.

For both exposures, we calculated unadjusted estimates assessing the differential uptake of microfinance by exposure. The first estimate is the crude average difference in the fraction of uptake of microfinance at the household level in the two exposure groups. The second estimate in the unaugmented GEE, which accounts for the correlation in outcomes among each village. In addition, we also developed a range of outcome models to be used as augmentation terms with the goal of reducing the estimated standard error[33]. For "Network Covariates Only," we include each of the variables mentioned in the simulation (estimates of $X^{(1)} - X^{(12)}$). For "Network & Sociodemographic," we include sex and age as well. For each strategy, β_0 is the estimated uptake of microfinance in the control group, and β_1 is the change associated with both exposures. Results are given in Table 6. Full details on the outcome models used for each exposure model and adjustment strategy can be found in the Supplementary Section S5.

	Est.	Adjustment	Estimate	S.E.	Wald	p-value
Exp. 1	β_0	Crude Estimate	0.209	0.019	11.207	<0.001
		Unadjusted GEE Estimate	0.249	0.043	5.761	<0.001
		Network Covariates Only	0.261	0.05	5.22	<0.001
		Network & Sociodemographic	0.215	0.019	11.11	<0.001
	β_1	Crude Estimate	-0.002	0.039	-0.055	0.478
		Unadjusted GEE Estimate	-0.069	0.058	-1.191	0.120
		Network Covariates Only	-0.199	0.06	-3.333	0.001
		Network & Sociodemographic	-0.137	0.031	-4.454	<0.001
Exp. 2	β_0	Crude Estimate	0.203	0.018	11.15	<0.001
		Unadjusted GEE Estimate	0.201	0.018	11.05	<0.001
		Network Covariates Only	0.208	0.018	11.37	<0.001
		Network & Sociodemographic	0.208	0.018	11.38	<0.001
	β_1	Crude Estimate	0.018	0.04	0.44	0.332
		Unadjusted GEE Estimate	0.03	0.038	0.79	0.216
		Network Covariates Only	0.045	0.041	1.08	0.143
		Network & Sociodemographic	0.045	0.041	1.08	0.143

Table 6: Estimates of the exposure effect on uptake of microfinance for several adjustment strategies. Exposure 1 is a village having a high fraction of village leaders, and Exposure 2 is a high fraction of participants using the self-help program. For each strategy, β_0 is the estimated uptake of microfinance in the control group.

Table 6 shows that adjusting for the propensity of exposure alters the estimated exposure effect. For example, the estimate for the effect of Exposure 1 changes from -0.002 to -0.069, and the estimated effect for Exposure 2 from 0.018 to 0.03. These moderately large changes are indicative of confounding by network features, and adjustment for exposure propensity is required. Additionally, adjusting for both network and sociodemographic covariates for Exposure 1 substantially reduces estimated standard error, and both augmentation models conclude an exposure effect not detected by the unadjusted analysis. In contrast, the analysis of Exposure 2 does not show an effect of micro-finance on uptake.

These empirical results can be compared to the related simulation setting. If the exposure model is correctly specified, no bias is expected; the adjustment strategy consisting of both Network and Sociodemographic covariates for the exposure of a high fraction of leaders reduces estimated standard error by 46%, comparable to the corresponding simulation scenario improvement in RMSE of 26-52%. It is possible that other measures of leadership for multilayered networks[35] would show further improvements in efficiency. In contrast, the analysis of the exposure of high rates of self-help does not improve estimated standard error, and fails to show an exposure effect. In the corresponding simulation scenario, the true difference due to the observational exposure is expected to be detected with high probability (as shown by the row showing high statistical power). Therefore, not detecting an exposure effect for self-help is either due to an improbable failure to detect significance, or that self-help is in fact not associated with taking up microfinance.

5 Discussion

In an epidemic process, infectious outcomes depend on contact network structure and spreading process dynamics. When assessing the marginal effect of exposure on the infectious process, one strategy to improve the estimation of the exposure effect is to adjust for covariate imbalance in the clusters in each exposure group. Several contact network features and characteristics of epidemic spread can be included to adjust this analysis. In this paper, we have used the augmented GEE for observational studies to estimate the magnitude of these gains, as well as investigated how these gains are modified by network properties and epidemic dynamics. We found that adjusting for baseline infections yields robust gains across each scenario, and that the extent of improvements depends on the specific aspects of the epidemic process.

We considered including augmentation terms that reduce network properties to a single covariate for each node. These covariates differed in the gains they provide in our simulation scenarios, but also in their usefulness across epidemic scenarios, interpretability, and feasibility of gathering in practice. For example, the sum of all inverse path lengths to an infected individual showed both wide variation in RMSE improvements across each setting. It would also be difficult to assess this covariate for each person in practice unless one obtains the full network and the infectious state of each individual at baseline. In contrast, each individuals' degree may be feasible to obtain, but the gains we observed from this covariate were modest. Averaged across all scenarios, the number of neighbors infected at baseline is an excellent covariate in each of these respects.

This work invites several extensions. We assumed that each collection of networks is known with perfect accuracy, which is not realistic. Information may be missing or misreported for individual outcomes, contact network data, or both, which may lead to bias or lowered power in estimating the exposure effect. In addition, out epidemic process and exposure regime may be a restrictively simple, failing to capture realistic dynamics of an epidemic under study.

Acknowledgements

We are grateful for support from NIH Grants 2T32AI007358-26 and R37 AI51164.

References

[1] Ove Frank and David Strauss. Markov graphs. *Journal of the American Statistical Association*, 81(395):832–842, 1986.

[2] P. Erdös and Alfréd. Rényi. The evolution of random graphs. *Publ. Math. Inst. Hung. Acad. Sci.*, 5:17–61, 1960.

[3] Albert-László Barabási and Réka Albert. Emergence of scaling in random networks. *Science*, 286:509–512, 1999.

[4] Duncan J. Watts and Steven H. Strogatz. Collective dynamics of 'small-world' networks. *Nature*, 393:440–442, 1998.

[5] M. E. J. Newman. *Networks: An Introduction*. Oxford University Press, Inc., New York, NY, USA, 2010.

[6] Tendani Gaolathe, Kathleen E Wirth, Molly Pretorius Holme, Joseph Makhema, Sikhulile Moyo, Unoda Chakalisa, Etienne Kadima Yankinda, Quanhong Lei, Mompati Mmalane, Vlad Novitsky, et al. Botswana's progress toward achieving the 2020 unaids 90-90-90 antiretroviral therapy and virological suppression goals: a population-based survey. *The Lancet HIV*, 2016.

[7] Richard Hayes, Helen Ayles, Nulda Beyers, Kalpana Sabapathy, Sian Floyd, Kwame Shanaube, Peter Bock, Sam Griffith, Ayana Moore, Deborah Watson-Jones, et al. Hptn 071 (popart): rationale and design of a cluster-randomised trial of the population impact of an hiv combination prevention intervention including universal testing and treatment-a study protocol for a cluster randomised trial. *Trials*, 15(1):57, 2014.

[8] G Chemie et al. Uptake of community-based hiv testing during a multi-disease health campaign in rural uganda. *PLoS One*, 9(1):e84317, 2014.

[9] Elihu Katz, Martin L Levin, and Herbert Hamilton. Traditions of research on the diffusion of innovation. *American Sociological Review*, pages 237–252, 1963.

[10] Paul R Rosenbaum. Observational studies. In *Observational Studies*, pages 1–17. Springer, 2002.

[11] P. R. Rosenbaum. *Design of Observational Studies*. Springer, New York.

[12] Michael G Hudgens and M Elizabeth Halloran. Toward causal inference with interference. *Journal of the American Statistical Association*, 2012.

[13] David M Murray. *Design and analysis of group-randomized trials*, volume 29. Oxford University Press, 1998.

[14] Sandra Eldridge and Sally Kerry. *A practical guide to cluster randomised trials in health services research*, volume 120. John Wiley & Sons, 2012.

[15] Patrick C Staples, Elizabeth L Ogburn, and Jukka-Pekka Onnela. Incorporating contact network structure in cluster randomized trials. *Scientific reports*, 5, 2015.

[16] Scott L Zeger and Kung-Yee Liang. Longitudinal data analysis for discrete and continuous outcomes. *Biometrics*, pages 121–130, 1986.

[17] Alan E Hubbard, Jennifer Ahern, Nancy L Fleischer, Mark Van der Laan, Sheri A Lippman, Nicholas Jewell, Tim Bruckner, and William A Satariano. To gee or not to gee: comparing population average and mixed models for estimating the associations between neighborhood risk factors and health. *Epidemiology*, 21(4):467–474, 2010.

[18] Anastasios A Tsiatis et al. Covariate adjustment for two-sample treatment comparisons in randomized clinical trials: A principled yet flexible approach. *Statistics in medicine*, 27(23):4658–4677, 2008.

[19] Mark J Van der Laan and Sherri Rose. *Targeted learning: causal inference for observational and experimental data*. Springer Science & Business Media, 2011.

[20] Carolyn J Anderson, Stanley Wasserman, and Katherine Faust. Building stochastic blockmodels. *Social Networks*, 14(1–2):137–161, 1992. Special Issue on Blockmodels.

[21] Brian Karrer and Mark EJ Newman. Stochastic blockmodels and community structure in networks. *Physical Review E*, 83(1):016107, 2011.

[22] Mark EJ Newman. Assortative mixing in networks. *Physical review letters*, 89(20):208701, 2002.

[23] Duncan S Callaway, John E Hopcroft, Jon M Kleinberg, Mark EJ Newman, and Steven H Strogatz. Are randomly grown graphs really random? *Physical Review E*, 64(4):041902, 2001.

[24] R Xulvi-Brunet and IM Sokolov. Reshuffling scale-free networks: From random to assortative. *Physical Review E*, 70(6):066102, 2004.

[25] A Ramachandra Rao, Rabindranath Jana, and Suraj Bandyopadhyay. A markov chain monte carlo method for generating random (0, 1)-matrices with given marginals. *Sankhyā: The Indian Journal of Statistics, Series A*, pages 225–242, 1996.

[26] Romualdo Pastor-Satorras, Claudio Castellano, Piet Van Mieghem, and Alessandro Vespignani. Epidemic processes in complex networks. *Rev. Mod. Phys.*, 87:925–979, Aug 2015.

[27] Roy M. Anderson and Robert M. May. *Infectious Diseases of Humans*. Oxford University Press, Oxford, U.K., 1991.

[28] Tao Zhou, Jian-Guo Liu, Wen-Jie Bai, Guanrong Chen, and Bing-Hong Wang. Behaviors of susceptible-infected epidemics on scale-free networks with identical infectivity. *Physical Review E*, 74(5):056109, 2006.

[29] James Woodward. Probabilistic causality, direct causes and counterfactual dependence. *Stochastic causality*, pages 39–63, 2001.

[30] Tobias Kurth, Alexander M Walker, Robert J Glynn, K Arnold Chan, J Michael Gaziano, Klaus Berger, and James M Robins. Results of multivariable logistic regression, propensity matching, propensity adjustment, and propensity-based weighting under conditions of nonuniform effect. *American Journal of Epidemiology*, 163(3):262–270, 2006.

[31] M. Prague, M. Houcine, L. Temime, and V. DeGruttola. Analysis of clustered observational data: application to the evaluation of stress and fatigue in french intensive-care registered nurses and nurses aides. 2016.

[32] Melanie Prague, Rui Wang, Alisa Stephens, Eric Tchetgen Tchetgen, and Victor DeGruttola. Accounting for interactions and complex inter-subject dependency in estimating treatment effect in cluster-randomized trials with missing outcomes. *Biometrics*, 2016.

[33] Alisa J Stephens, Eric J Tchetgen Tchetgen, and Victor De Gruttola. Augmented gee for improving efficiency and validity of estimation in cluster randomized trials by leveraging cluster-and individual-level covariates. *Statistics in medicine*, 31(10):915, 2012.

[34] RI Jennrich and PF Sampson. Application of stepwise regression to non-linear estimation. *Technometrics*, 10(1):63–72, 1968.

[35] Elisa Omodei and Alex Arenas. Untangling the role of diverse social dimensions in the diffusion of microfinance. *arXiv preprint arXiv:1609.01455*, 2016.

[36] Azra C Ghani and Geoffrey P Garnett. Risks of acquiring and transmitting sexually transmitted diseases in sexual partner networks. *Sexually transmitted diseases*, 27(10):579–587, 2000.

[37] Abhijit Banerjee, Arun G Chandrasekhar, Esther Duflo, and Matthew O Jackson. The diffusion of microfinance. *Science*, 341(6144):1236498, 2013.

Supplementary Material

In this supplement, we give additional details on given in the main paper. In Section S1, we provide two figures that illustrate the epidemic spreading process through each network, as well as the infectious process over time. In Section S2, we specify the block structure used in the simulated epidemic process. In Section S3, we give tables of the statistical properties of the simulation results considering all simulation aspects. In Section S4, we provide an analysis of which features are selected in the stepwise procedure for each simulation scenario. In Section S5, we provide details on the degree distribution and outcome models used to improve analysis in the application of the augmented GEE to the diffusion of microfinance in Karnataka, India.

S1: Figures of the Infectious Process

Figure 4 shows a schematic of infectious process for a specific node in a given network. Figure 5 shows the infectious process at its onset, its development until baseline, and its progression until study end.

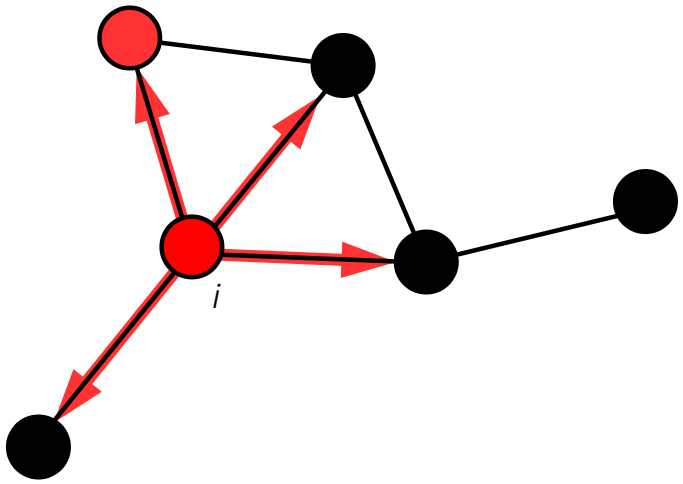

Figure 4: A schematic of the stochastic agent-based infectious process. Node j is shown in network or cluster i. Infected nodes are shown in red, and susceptible nodes are black. Individual j is connected to $k_{i;j} = 4$ other nodes. Because j is infected, they may infect $q_{i;j}$ of their neighbors at each time step.

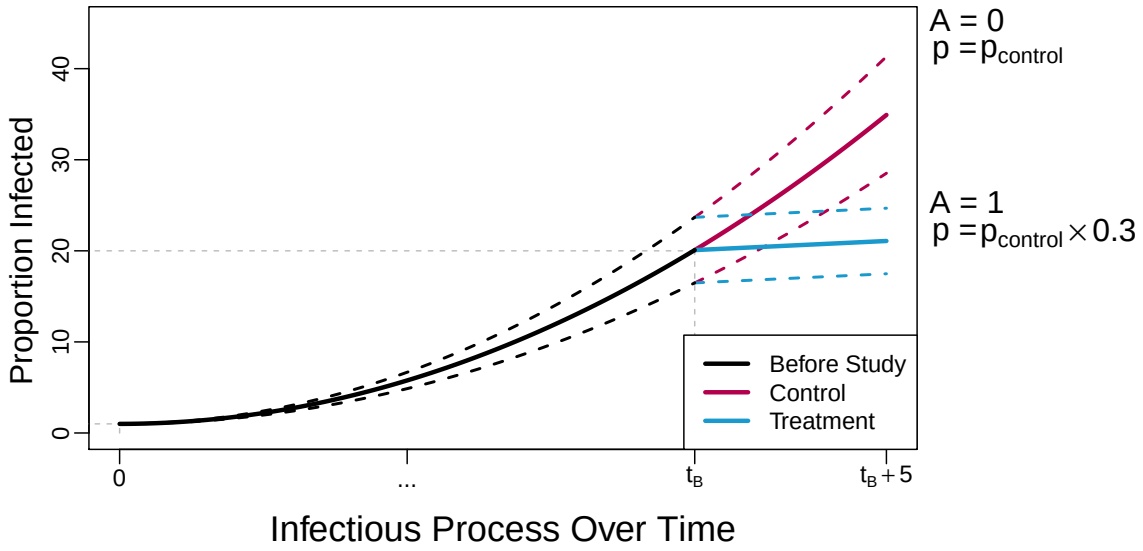

Figure 5: S% of nodes are randomly selected as initially infected, and an infectious process spreads until B% overall baseline prevalence is reached (time t_{B}). In this figure, $S = 1$ and $B = 20$. Individuals are infected according to Algorithm 2 in the paper. Then, each cluster is randomly assigned to be exposed ($A_i = 1$) or unexposed ($A_i = 0$), wherein infected nodes in treated clusters have their infection probability reduced by a multiplicative factor of $1/3$. The process continues for another $T = 5$ time steps.

S2: Generation of Block Structure

In order to simulate epidemic spread, we create a collection of networks designed to mimic community structure and mixing patterns found in sexual contact networks. To accomplish this, we employ the Degree-Corrected Stochastic Blockmodel[1], which allows for an arbitrary degree distribution and block structure.

We create networks that are bipartite, show community structure, and allow for members of two blocks to mix more than other block pairs. Let $b_i \in \{1, ..., B\}$ be the block membership for node i, with $B = 8$ blocks total. Define the total degree for members of each block i as $\kappa_j := \sum_i k_i \mathbb{I}(b_i = j)$, and the total number of edges $m = \frac{\sum_{j=1}^{B} \kappa_j}{2}$. The Degree-Corrected Stochastic Blockmodel specifies the amount of mixing between blocks by specifying mixing matrix $\omega \in \mathbb{N}^{B \times B}$, which details the total number of edges shared between members of pairs of blocks. This matrix requires a constraint to ensure all edges belong to some block pair: $\omega \mathbf{1} \equiv \boldsymbol{\kappa}$, where $\mathbf{1} = \{1, ..., 1\}^\top$ and $\boldsymbol{\kappa} = \{\kappa_1, ..., \kappa_B\}^\top$.

Before specifying the mixing structure we chose for our paper, we introduce three consistent mixing matrix specifications, each with different properties we detail next. Edges might exist only between the two halves of the network, making it a *bipartite* network. In order to create consistent bipartite networks, we define the two halves as four blocks each, $\mathcal{J}_1 = \{1, 2, 3, 4\}$ and $\mathcal{J}_2 = \{5, 6, 7, 8\}$. We require the total number of edges existing between the four blocks of each half of the bipartition to be equal:

$$\sum_{i \in \mathcal{J}_1} \kappa_i \equiv \sum_{j \in \mathcal{J}_2} \kappa_j \tag{7}$$

If edges only exist between pairs of blocks (κ_i, κ_j), the networks is said to comprise *bipartite communities*. $\omega_{\text{community}}$ gives the mixing matrix corresponding to edges only existing in four bipartite communities. It is also possible for only some block pairs to represent a sociodemographic group that mixes less discriminately with other blocks. For example, in the context of HIV, such blocks may stand to represent sex workers. This is accomplished by those blocks sharing edges proportional to the degree of the blocks in the other bipartite half: this is specified by $\omega_{\text{sexworker}}$. Finally, all blocks in each bipartite half may share their edges proportional to the total degree of each other block in the other bipartition half, which is detailed by ω_{random}. Each of these mixing matrices are detailed below.

$$\omega_{\text{community}} = \begin{bmatrix} 0 & 0 & 0 & 0 & \kappa_1 & 0 & 0 & 0 \\ 0 & 0 & 0 & 0 & 0 & \kappa_2 & 0 & 0 \\ 0 & 0 & 0 & 0 & 0 & 0 & \kappa_3 & 0 \\ 0 & 0 & 0 & 0 & 0 & 0 & 0 & \kappa_4 \\ \kappa_5 & 0 & 0 & 0 & 0 & 0 & 0 & 0 \\ 0 & \kappa_6 & 0 & 0 & 0 & 0 & 0 & 0 \\ 0 & 0 & \kappa_7 & 0 & 0 & 0 & 0 & 0 \\ 0 & 0 & 0 & \kappa_8 & 0 & 0 & 0 & 0 \end{bmatrix}$$

$$\omega_{\text{sexworker}} = \begin{bmatrix} 0 & 0 & 0 & 0 & \frac{\kappa_1\kappa_5}{2m} & \frac{\kappa_1\kappa_6}{2m} & \frac{\kappa_1\kappa_7}{2m} & \frac{\kappa_1\kappa_8}{2m} \\ 0 & 0 & 0 & 0 & \frac{\kappa_1\kappa_6}{2m} & \kappa_2 - \frac{\kappa_1\kappa_6}{2m} & 0 & 0 \\ 0 & 0 & 0 & 0 & \frac{\kappa_1\kappa_7}{2m} & 0 & \kappa_3 - \frac{\kappa_1\kappa_7}{2m} & 0 \\ 0 & 0 & 0 & 0 & \frac{\kappa_1\kappa_8}{2m} & 0 & 0 & \kappa_4 - \frac{\kappa_1\kappa_8}{2m} \\ \frac{\kappa_5\kappa_1}{2m} & \frac{\kappa_5\kappa_1}{2m} & \frac{\kappa_5\kappa_3}{2m} & \frac{\kappa_5\kappa_4}{2m} & 0 & 0 & 0 & 0 \\ \frac{\kappa_5\kappa_2}{2m} & \kappa_6 - \frac{\kappa_5\kappa_2}{2m} & 0 & 0 & 0 & 0 & 0 & 0 \\ \frac{\kappa_5\kappa_3}{2m} & 0 & \kappa_7 - \frac{\kappa_5\kappa_3}{2m} & 0 & 0 & 0 & 0 & 0 \\ \frac{\kappa_5\kappa_4}{2m} & 0 & 0 & \kappa_8 - \frac{\kappa_5\kappa_4}{2m} & 0 & 0 & 0 & 0 \end{bmatrix}$$

$$\omega_{\text{random}} = \begin{bmatrix} 0 & 0 & 0 & 0 & \frac{\kappa_1\kappa_5}{2m} & \frac{\kappa_1\kappa_6}{2m} & \frac{\kappa_1\kappa_7}{2m} & \frac{\kappa_1\kappa_8}{2m} \\ 0 & 0 & 0 & 0 & \frac{\kappa_2\kappa_5}{2m} & \frac{\kappa_2\kappa_6}{2m} & \frac{\kappa_2\kappa_7}{2m} & \frac{\kappa_2\kappa_8}{2m} \\ 0 & 0 & 0 & 0 & \frac{\kappa_3\kappa_5}{2m} & \frac{\kappa_3\kappa_6}{2m} & \frac{\kappa_3\kappa_7}{2m} & \frac{\kappa_3\kappa_8}{2m} \\ 0 & 0 & 0 & 0 & \frac{\kappa_4\kappa_5}{2m} & \frac{\kappa_4\kappa_6}{2m} & \frac{\kappa_4\kappa_7}{2m} & \frac{\kappa_4\kappa_8}{2m} \\ \frac{\kappa_5\kappa_1}{2m} & \frac{\kappa_5\kappa_2}{2m} & \frac{\kappa_5\kappa_3}{2m} & \frac{\kappa_5\kappa_4}{2m} & 0 & 0 & 0 & 0 \\ \frac{\kappa_6\kappa_1}{2m} & \frac{\kappa_6\kappa_2}{2m} & \frac{\kappa_6\kappa_3}{2m} & \frac{\kappa_6\kappa_4}{2m} & 0 & 0 & 0 & 0 \\ \frac{\kappa_7\kappa_1}{2m} & \frac{\kappa_7\kappa_2}{2m} & \frac{\kappa_7\kappa_3}{2m} & \frac{\kappa_7\kappa_4}{2m} & 0 & 0 & 0 & 0 \\ \frac{\kappa_8\kappa_1}{2m} & \frac{\kappa_8\kappa_2}{2m} & \frac{\kappa_8\kappa_3}{2m} & \frac{\kappa_8\kappa_4}{2m} & 0 & 0 & 0 & 0 \end{bmatrix}$$

Finally, a range of linear combinations of these matrices may be used to specify a mixing matrix with a combination of features described above, provided these combinations sum to 1:

$$\omega = \lambda \cdot \omega_{\text{community}} + \mu \cdot \omega_{\text{sexworker}} + (1 - \lambda - \mu) \cdot \omega_{\text{random}} \tag{8}$$

To create a random bipartite comunity structure, we selected mixing matrix values $(\lambda = 0.0, \mu = 0.0)$. To create strong community structure, two highly-mixing blocks, and some random mixing between blocks, we selected mixing matrix values $(\lambda = 0.1, \mu = 0.8)$.

S3: Full Simulation Results

In this section, we show the empirical correlations between each network feature with the exposure as well as the outcome. We also give tables for the exposure effect size, bias, estimated and robust standard error, reduction in RMSE, statistical power, and statistical coverage. For $r = 1, ..., R$ trials, we compute the augmented GEE estimates of treatment effect size $\widehat{\beta}_r$ and estimate standard deviation $\widehat{\text{sd}}_r(\widehat{\beta}_r)$. In addition, we use trial outcomes $Y_{ij;r}$ to compute the true treatment effect by calculating the average risk difference across all trials:

$$\beta^* := \frac{\sum_{ijr} Y_{ij;r} \cdot \mathbb{I}(A_i = 1)}{\sum_{ijr} \mathbb{I}(A_i = 1)} - \frac{\sum_{ijr} Y_{ij;r} \cdot \mathbb{I}(A_i = 0)}{\sum_{ijr} \mathbb{I}(A_i = 0)} \tag{9}$$

From this value, obtain the estimated empirical bias and empirical variance of the treatment effect estimate:

$$\widehat{\text{Bias}}_r(\widehat{\beta_r}) = \beta^* - \widehat{\beta_r} \tag{10}$$

To combine the amount of bias and size of the standard error in a single composite measure, we compute the root mean squared error for each trial, defined as:

$$\widehat{\text{RMSE}} := \sqrt{\frac{1}{R} \sum_r \widehat{\text{Bias}}_r(\widehat{\beta}_r)^2 + \widehat{\text{Var}}(\widehat{\beta})} \tag{11}$$

Our metric for the gained improvement by the augmentation term is the percent reduction in RMSE for each adjustment covariate set, comparing the augmentation adjustment $\widehat{\text{RMSE}}_{\text{adj}}$ to that of the unadjusted GEE ($\widehat{\text{RMSE}}_{\text{GEE}}$:

$$\widehat{\text{Gain}} := 100 \times \left(1 - \frac{\widehat{\text{RMSE}}_{\text{adj}}}{\widehat{\text{RMSE}}_{\text{GEE}}}\right) \tag{12}$$

Statistical coverage is the probability that the estimated confidence intervals cover the true treatment effect, which must be 95% or greater for valid inference:

$$P(\beta_A^* \in CI(\hat{\beta}^*)) \tag{13}$$

Finally, in our setting with the null hypothesis $\beta = 0$, power is the probability that the confidence interval is significantly different from zero given that the treatment effect is not zero:

$$P(0 \notin CI(\hat{\beta}_A^*) | \beta_A \neq 0) \tag{14}$$

We show tables for these values in three views: averaged across all scenarios; modifications associated with altering one scenario holding all others constant; values conditional on the specific scenario considered.

Empirical Correlation in Generated Studies

Figure 6 gives the empirical correlation in our generated studies between the outcome and each covariate, as well as with the exposure. Nonzero covariate correlations in both panels suggests gains in efficiency when estimating the effect of exposure.

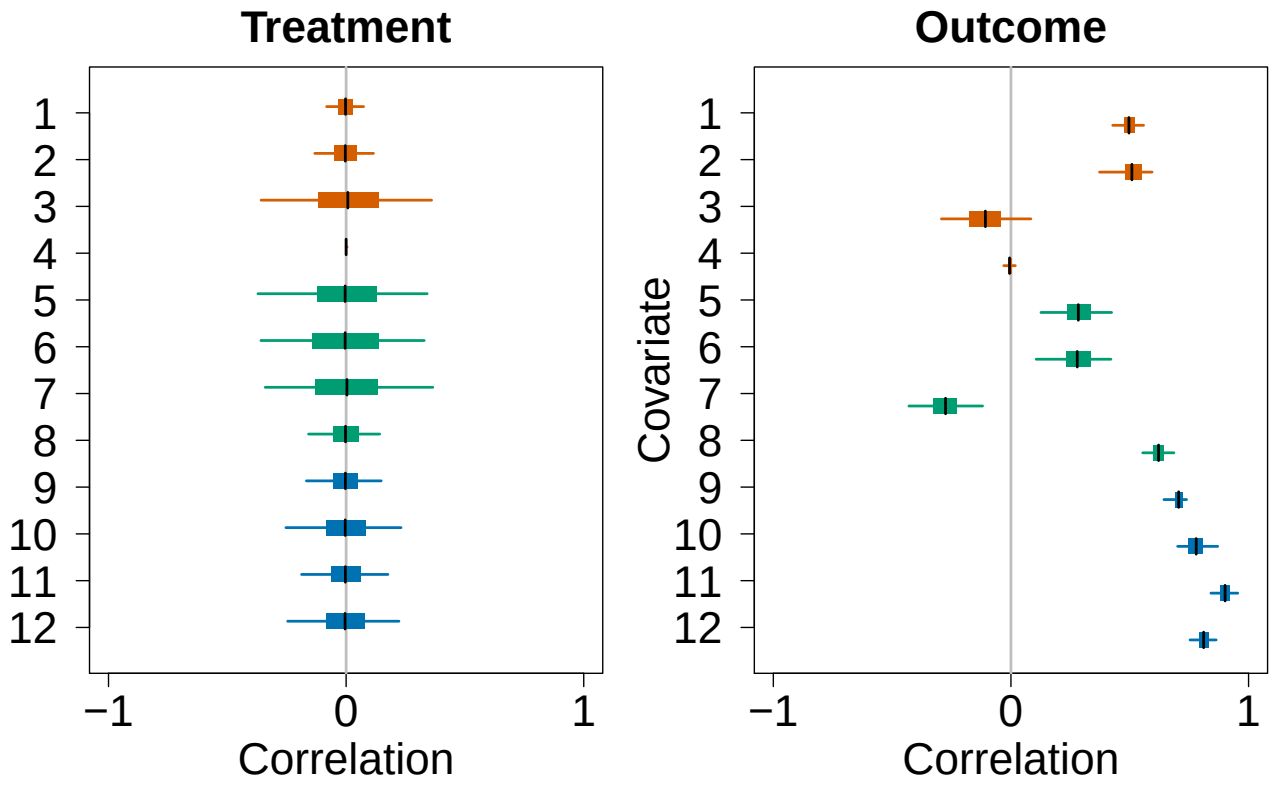

Figure 6: A plot of the distribution of univariate correlations between single covariates and indicators for either exposure or outcome. The left shows correlations with variation around zero, suggesting imperfect randomization due to finite sample sizes, and the right panel shows that some network or baseline epidemic covariates are correlated with the outcome.

Marginal Statistics Across All Scenarios

Table 7 presents the metrics averaged across all 2^6 simulation scenarios. Each column shows results for each of several adjustment strategies: including no adjustment covariates, $X^{(9)}$ only, all network covariates, and a stepwise selection of these covariates.

Exposure Effect $\overline{\beta}$: -3.23

	None	Only $X^{(9)}$	All	Step
Bias	0	0.08	0.11	0.1
SE	1.68	0.84	0.6	0.6
Empirical SE	1.39	0.7	0.64	0.63
Improvement	0(0)	43(23)	42(31)	43(30)
Power	48.1	90.9	94.3	94.2
Coverage	98(2)	97(2)	92(4)	92(4)

Table 7: An assortment of statistics averaged across all combinations of scenarios considered.

None: No adjustment term
$X^{(1)}$: Degree
$X^{(2)}$: Mean Neighbor Degree
$X^{(3)}$: Assortativity
$X^{(4)}$: Member of Connected Block
$X^{(5)}$: Size of Largest Component
$X^{(6)}$: Mean Component Size
$X^{(7)}$: Number of Components
$X^{(8)}$: Size of Node's Component
$X^{(9)}$: Total Neighbor Infections at baseline
$X^{(10)}$: Total Node's Component Infections at baseline
$X^{(11)}$: 1/nearest infected path length at baseline
$X^{(12)}$: $\sum_i$ 1/path length to Infected Node i at baseline
All: Complete inclusion of the above
Step: Stepwise regression of the above

$\mathbf{a} =$ [$\mathbb{I}$(High Degree),
$\mathbb{I}$(Powerlaw),
$\mathbb{I}$(Assortativity),
$\mathbb{I}$(Blocks),
$\mathbb{I}$(Degree Infectivity),
$\mathbb{I}$(High Baseline)]

Statistics Modification By Simulation Aspect

In this subsection, we present the change in each statistical performance metric changes when changing a single simulation aspect, holding all others constant. We estimate this by performing simple linear regression, with each metric as the outcome, and indicator variables for each simulation aspect as binary covariates. These estimates differ by the covariate set used in the augmentation term. for adjustment Tables 8-14 present these coefficients for exposure effect size, bias, estimated effect estimate standard error, empirical effect estimate standard error, improvement in RMSE, power, and coverage.

a	γ_a
(Intercept)	0.33
High Degree	-0.00
Powerlaw	-2.27
Assortative	0.01
Communities	-0.16
Degree Infectivity	-3.00
High Baseline	-0.52

Table 8: The average difference in exposure effect size associated with simulation aspect being 1 compared to 0, holding all other aspects constant.

Bias

	None	Only $X^{(9)}$	All	Step
(Intercept)	-0.00	0.11	0.20	0.19
High Degree	0.00	-0.09	-0.12	-0.12
Powerlaw	0.00	0.09	0.08	0.08
Assortative	0.00	-0.03	-0.05	-0.06
Communities	-0.00	0.01	0.03	0.04
Degree Infectivity	0.00	0.09	0.19	0.20
High Baseline	0.00	-0.13	-0.31	-0.30

Table 9: The average difference in exposure effect bias associated with simulation aspect being 1 compared to 0, holding all other aspects constant.

Robust S.E.

	None	Only $X^{(9)}$	All	Step
(Intercept)	0.75	0.16	0.11	0.10
High Degree	0.18	0.39	0.34	0.34
Powerlaw	0.28	0.30	0.14	0.13
Assortative	-0.05	-0.06	-0.06	-0.05
Communities	-0.17	-0.05	-0.04	-0.03
Degree Infectivity	0.90	0.42	0.47	0.47
High Baseline	0.72	0.36	0.14	0.14

Table 10: The average difference in the robust estimate of the exposure effect standard error associated with simulation aspect being 1 compared to 0, holding all other aspects constant.

Empirical S.E.

	None	Only $X^{(9)}$	All	Step
(Intercept)	0.42	0.17	0.23	0.22
High Degree	0.31	0.32	0.32	0.31
Powerlaw	0.14	0.20	0.12	0.13
Assortative	-0.03	-0.02	-0.06	-0.06
Communities	-0.04	-0.03	-0.04	-0.04
Degree Infectivity	0.56	0.38	0.40	0.41
High Baseline	0.99	0.20	0.08	0.07

Table 11: The average difference in empirical exposure effect standard error associated with simulation aspect being 1 compared to 0, holding all other aspects constant.

Improvement

	None	Only $X^{(9)}$	All	Step
(Intercept)	-0	41	15	18
High Degree	0	-13	-2	-3
Powerlaw	0	-16	1	-0
Assortative	0	5	8	7
Communities	-0	1	5	5
Degree Infectivity	0	1	-0	-1
High Baseline	0	27	44	42

Table 12: The average difference in the reduction of standard error associated with simulation aspect being 1 compared to 0, holding all other aspects constant.

Power

	None	Only $X^{(9)}$	All	Step
(Intercept)	31	96	95	94
High Degree	39	-4	-2	-2
Powerlaw	5	-3	2	2
Assortative	1	3	2	2
Communities	6	1	2	2
Degree Infectivity	-1	-2	-3	-2
High Baseline	-15	-5	-2	-2

Table 13: The average difference in the statistical power associated with simulation aspect being 1 compared to 0, holding all other aspects constant.

Coverage

	None	Only $X^{(9)}$	All	Step
(Intercept)	99	95	88	88
High Degree	-1	2	3	3
Powerlaw	0	1	1	-0
Assortative	-0	0	-1	-1
Communities	-0	0	1	1
Degree Infectivity	1	1	3	3
High Baseline	-3	1	2	2

Table 14: The average difference in the statistical coverage associated with simulation aspect being 1 compared to 0, holding all other aspects constant.

Statistics Conditional On Each Scenario

This subsection presents the performance metrics defined above for each simulation scenario.

a	β_a
000000	-0.25
000001	-2.30
000010	-1.22
000011	-3.46
000100	-0.34
000101	-2.48
000110	-1.35
000111	-3.62
001000	-0.32
001001	-2.37
001010	-1.13
001011	-3.23
001100	-0.42
001101	-2.09
001110	-1.19
001111	-3.08
010000	-0.79
010001	-3.50
010010	-5.29
010011	-3.68
010100	-0.75
010101	-3.60
010110	-5.14
010111	-3.43
011000	-0.77
011001	-3.87
011010	-4.94
011011	-3.55
011100	-0.83
011101	-3.64
011110	-4.73
011111	-3.43
100000	-2.07
100001	-3.84
100010	-6.76
100011	-3.63
100100	-2.23
100101	-4.27
100110	-6.60
100111	-3.70
101000	-2.06
101001	-4.25
101010	-6.73
101011	-3.27
101100	-2.17
101101	-3.91
101110	-6.51
101111	-3.77
110000	-1.68
110001	-4.25
110010	-5.79
110011	-3.02
110100	-1.77
110101	-4.00
110110	-5.90
110111	-3.14
111000	-1.92
111001	-4.29
111010	-6.02
111011	-3.55
111100	-1.75
111101	-3.70
111110	-6.05
111111	-3.42

$$\mathbf{a} = [\mathbb{I}(\text{High Degree}), \mathbb{I}(\text{Powerlaw}), \mathbb{I}(\text{Assortativity}), \mathbb{I}(\text{Heterogeneous Block Structure}), \mathbb{I}(\text{Degree Infectivity}), \mathbb{I}(\text{High Baseline})]$$

Table 15: The true effect size for each exposure scenario, measured in percentage points.

Bias

	None	Only $X^{(9)}$	All	Step
000000	0	0.10	0.30	0.30
000001	0	0.00	-0.10	-0.10
000010	0	0.20	0.40	0.30
000011	0	0.00	0.00	0.00
000100	0	0.10	0.30	0.30
000101	0	-0.10	-0.20	-0.20
000110	0	0.20	0.40	0.40
000111	0	-0.10	-0.10	0.00
001000	0	0.10	0.30	0.30
001001	0	-0.10	-0.20	-0.20
001010	0	0.30	0.40	0.40
001011	0	0.10	0.10	0.10
001100	0	0.00	0.20	0.10
001101	0	0.10	0.10	0.10
001110	0	0.10	0.30	0.30
001111	0	0.20	0.30	0.30
010000	0	0.20	0.00	0.00
010001	0	0.10	-0.20	-0.20
010010	0	0.50	0.90	0.90
010011	0	0.00	0.00	0.00
010100	0	0.00	0.10	0.10
010101	0	0.20	0.10	0.10
010110	0	0.40	0.70	0.70
010111	0	0.30	0.30	0.30
011000	0	0.10	0.20	0.20
011001	0	0.00	-0.20	-0.20
011010	0	0.30	0.50	0.50
011011	0	0.00	-0.10	-0.10
011100	0	0.10	0.10	0.10
011101	0	0.20	0.10	0.10
011110	0	0.10	0.20	0.20
011111	0	0.20	0.20	0.20
100000	0	0.10	0.10	0.10
100001	0	0.10	0.10	0.10
100010	0	0.10	0.30	0.30
100011	0	-0.10	-0.10	-0.10
100100	0	0.00	0.00	0.00
100101	0	-0.20	-0.30	-0.30
100110	0	0.10	0.20	0.20
100111	0	-0.20	-0.30	-0.30
101000	0	0.10	0.10	0.10
101001	0	-0.30	-0.30	-0.30
101010	0	0.00	0.10	0.10
101011	0	0.00	0.00	0.00
101100	0	0.00	0.00	0.00
101101	0	0.10	0.00	0.00
101110	0	0.10	0.10	0.10
101111	0	-0.20	-0.30	-0.30
110000	0	0.20	0.10	0.10
110001	0	-0.20	-0.30	-0.30
110010	0	0.20	0.50	0.50
110011	0	0.30	0.30	0.30
110100	0	0.00	0.00	0.00
110101	0	0.00	0.00	0.00
110110	0	0.30	0.60	0.60
110111	0	0.10	0.10	0.10
111000	0	0.00	0.00	0.00
111001	0	-0.30	-0.40	-0.50
111010	0	0.20	0.40	0.40
111011	0	-0.10	-0.30	-0.30
111100	0	0.10	0.10	0.10
111101	0	0.20	0.20	0.20
111110	0	0.20	0.40	0.40
111111	0	0.00	0.00	0.00

Table 16: The average estimated bias in estimates for each exposure scenario, measured in percentage points.

Robust Standard Error

	None	Only $X^{(9)}$	All Step
000000	0.70	0.20	0.20 0.20
000001	1.60	0.60	0.30 0.30
000010	1.40	0.50	0.40 0.40
000011	1.90	0.50	0.40 0.40
000100	0.70	0.20	0.20 0.20
000101	1.60	0.60	0.30 0.30
000110	1.20	0.40	0.40 0.40
000111	1.80	0.50	0.40 0.40
001000	0.80	0.20	0.20 0.20
001001	1.50	0.60	0.30 0.30
001010	1.30	0.40	0.40 0.40
001011	1.60	0.50	0.30 0.30
001100	0.80	0.20	0.20 0.20
001101	1.50	0.60	0.30 0.30
001110	1.20	0.40	0.40 0.40
001111	1.60	0.50	0.30 0.40
010000	0.70	0.40	0.30 0.30
010001	1.90	1.20	0.60 0.60
010010	2.80	1.40	1.10 1.10
010011	2.90	0.80	0.50 0.50
010100	0.60	0.40	0.30 0.30
010101	1.70	1.10	0.50 0.50
010110	2.40	1.30	1.00 1.00
010111	2.20	0.80	0.50 0.50
011000	0.80	0.40	0.30 0.30
011001	2.10	0.90	0.50 0.50
011010	2.60	1.50	0.90 0.90
011011	2.70	0.70	0.50 0.50
011100	0.60	0.20	0.20 0.20
011101	1.80	0.90	0.40 0.40
011110	1.90	1.10	0.80 0.80
011111	2.10	0.70	0.40 0.40
100000	0.70	0.30	0.30 0.30
100001	1.80	0.80	0.50 0.50
100010	1.90	1.10	0.90 0.90
100011	2.60	1.60	1.40 1.40
100100	0.70	0.30	0.30 0.30
100101	1.80	0.80	0.50 0.50
100110	1.80	1.00	0.80 0.80
100111	2.70	1.60	1.40 1.40
101000	0.70	0.40	0.30 0.30
101001	1.90	0.80	0.50 0.50
101010	2.10	1.10	0.90 0.90
101011	2.50	1.50	1.30 1.30
101100	0.70	0.30	0.30 0.30
101101	1.90	0.90	0.50 0.50
101110	1.80	1.10	0.80 0.80
101111	2.50	1.60	1.40 1.40
110000	0.70	0.50	0.40 0.40
110001	1.80	1.50	0.60 0.60
110010	2.40	1.20	1.10 1.10
110011	2.70	1.70	1.40 1.40
110100	0.60	0.50	0.30 0.30
110101	1.70	1.30	0.60 0.60
110110	2.20	1.10	0.90 0.90
110111	2.40	1.70	1.40 1.40
111000	0.70	0.40	0.30 0.30
111001	1.90	1.20	0.50 0.50
111010	2.20	1.20	1.00 1.00
111011	2.60	1.60	1.30 1.30
111100	0.70	0.30	0.30 0.30
111101	1.80	1.10	0.50 0.50
111110	1.90	1.10	0.90 0.90
111111	2.30	1.50	1.20 1.20

Table 17: The average estimated robust standard error for each exposure scenario, measured in percentage points.

Empirical Standard Error

	None	Only $X^{(9)}$	All Step
000000	0.30	0.20	0.50 0.50
000001	1.30	0.40	0.40 0.40
000010	0.80	0.40	0.40 0.40
000011	1.60	0.50	0.30 0.30
000100	0.30	0.10	0.50 0.50
000101	1.50	0.50	0.30 0.30
000110	0.80	0.40	0.50 0.40
000111	1.40	0.50	0.40 0.30
001000	0.40	0.20	0.30 0.30
001001	1.40	0.50	0.30 0.30
001010	0.90	0.40	0.50 0.50
001011	1.50	0.50	0.40 0.40
001100	0.90	0.20	0.40 0.40
001101	1.50	0.50	0.30 0.30
001110	0.70	0.40	0.50 0.50
001111	1.60	0.40	0.30 0.30
010000	0.40	0.40	0.30 0.40
010001	1.80	0.90	0.60 0.60
010010	1.40	0.80	0.90 0.90
010011	2.50	0.80	0.60 0.60
010100	0.40	0.40	0.30 0.30
010101	1.70	0.70	0.60 0.60
010110	1.40	1.00	0.80 0.80
010111	2.10	0.70	0.60 0.60
011000	0.60	0.60	0.40 0.40
011001	1.80	0.70	0.50 0.50
011010	1.90	1.30	0.90 0.90
011011	1.90	0.60	0.50 0.50
011100	0.40	0.20	0.30 0.30
011101	1.60	0.60	0.50 0.50
011110	1.10	0.90	0.70 0.70
011111	1.60	0.70	0.50 0.50
100000	0.50	0.30	0.30 0.30
100001	1.90	0.60	0.50 0.50
100010	1.40	0.90	1.10 1.10
100011	2.50	1.30	1.20 1.20
100100	0.50	0.30	0.40 0.30
100101	1.90	0.60	0.60 0.60
100110	1.40	1.00	0.90 0.90
100111	2.70	1.30	1.20 1.20
101000	0.50	0.40	0.40 0.30
101001	2.00	0.60	0.60 0.50
101010	1.20	0.90	0.90 0.90
101011	2.20	1.20	1.20 1.20
101100	0.40	0.30	0.30 0.30
101101	1.70	0.60	0.50 0.50
101110	2.10	1.60	1.00 1.00
101111	2.30	1.30	1.10 1.10
110000	0.60	0.60	0.50 0.50
110001	1.80	0.90	0.70 0.60
110010	1.80	1.00	1.20 1.20
110011	2.20	1.50	1.60 1.60
110100	0.50	0.70	0.30 0.30
110101	1.70	0.90	0.60 0.60
110110	1.90	0.80	0.90 1.00
110111	1.90	1.30	1.30 1.30
111000	0.50	0.40	0.30 0.30
111001	2.20	0.90	0.50 0.50
111010	1.00	0.90	1.10 1.10
111011	2.30	1.30	1.10 1.10
111100	0.50	0.40	0.30 0.30
111101	1.90	0.70	0.60 0.60
111110	1.00	0.80	1.00 1.00
111111	2.30	1.20	1.20 1.20

Table 18: The average empirical standard error for each exposure scenario, measured in percentage points.

Improvement

	None	Only $X^{(9)}$	All	Step
000000	0	46	-78	-66
000001	0	65	68	69
000010	0	45	25	26
000011	0	68	78	78
000100	0	55	-66	-57
000101	0	64	78	78
000110	0	44	29	31
000111	0	67	75	75
001000	0	55	-0	5
001001	0	67	74	73
001010	0	50	30	31
001011	0	68	75	75
001100	0	82	51	54
001101	0	67	75	75
001110	0	47	20	22
001111	0	69	75	75
010000	0	-2	20	17
010001	0	50	63	63
010010	0	29	7	8
010011	0	67	76	76
010100	0	5	21	24
010101	0	54	65	65
010110	0	27	26	27
010111	0	61	70	69
011000	0	8	34	36
011001	0	61	73	72
011010	0	29	47	47
011011	0	65	74	74
011100	0	39	28	29
011101	0	62	67	67
011110	0	22	34	35
011111	0	58	66	66
100000	0	36	34	34
100001	0	68	75	74
100010	0	32	20	20
100011	0	47	51	51
100100	0	35	31	32
100101	0	64	65	65
100110	0	31	32	32
100111	0	52	54	54
101000	0	15	20	23
101001	0	64	68	70
101010	0	29	24	24
101011	0	46	44	44
101100	0	33	33	34
101101	0	63	71	71
101110	0	26	52	52
101111	0	44	50	50
110000	0	-3	17	17
110001	0	47	60	60
110010	0	44	31	31
110011	0	29	25	25
110100	0	-52	36	35
110101	0	49	67	67
110110	0	55	42	42
110111	0	31	31	31
111000	0	28	35	34
111001	0	55	69	69
111010	0	13	-11	-11
111011	0	42	50	50
111100	0	22	36	36
111101	0	61	68	68
111110	0	20	-9	-9
111111	0	47	49	49

Table 19: The average reduction in the RMSE using the adjusted GEE for each exposure scenario, measured in percentage points.

Power

	None	Only $X^{(9)}$	All	Step
000000	0	66	65	62
000001	25	100	100	100
000010	1	97	100	100
000011	46	100	100	100
000100	0	87	78	81
000101	33	97	100	100
000110	3	98	100	100
000111	57	100	100	100
001000	1	79	76	75
001001	33	98	100	100
001010	1	97	97	97
001011	55	100	100	100
001100	0	74	84	80
001101	24	98	100	100
001110	0	94	98	98
001111	49	100	100	100
010000	8	72	76	76
010001	45	93	100	100
010010	48	100	99	100
010011	15	100	100	100
010100	16	64	90	88
010101	58	96	100	100
010110	66	100	100	100
010111	31	100	100	100
011000	3	80	92	95
011001	41	100	100	100
011010	46	96	100	100
011011	20	100	100	100
011100	13	94	100	99
011101	53	99	100	100
011110	82	100	100	100
011111	38	100	100	100
100000	93	99	99	99
100001	58	99	100	100
100010	100	100	100	100
100011	24	69	76	76
100100	97	100	100	100
100101	68	100	100	100
100110	100	100	100	100
100111	27	64	72	71
101000	94	100	100	100
101001	60	99	100	100
101010	99	100	100	100
101011	20	63	65	67
101100	99	100	100	100
101101	56	100	100	100
101110	99	99	100	100
101111	34	71	75	76
110000	72	91	99	99
110001	67	83	100	100
110010	86	100	100	100
110011	10	55	66	65
110100	91	95	100	100
110101	66	93	100	100
110110	94	100	100	100
110111	20	48	69	68
111000	86	100	100	100
111001	65	94	100	100
111010	97	100	100	100
111011	23	60	74	76
111100	84	99	100	100
111101	49	96	100	100
111110	97	100	100	100
111111	30	61	86	87

Table 20: The average statistical power for each exposure scenario, measured in percentage points.

Coverage

	None	Only $X^{(9)}$	All	Step
000000	100	92	87	85
000001	99	100	88	89
000010	98	94	88	88
000011	99	95	96	95
000100	100	95	80	81
000101	97	96	95	95
000110	98	97	87	87
000111	100	97	96	98
001000	99	91	83	83
001001	95	96	93	93
001010	100	98	81	83
001011	95	95	92	93
001100	99	98	89	91
001101	96	98	92	93
001110	99	94	85	87
001111	96	93	91	92
010000	99	95	93	92
010001	97	96	92	90
010010	100	100	92	93
010011	100	93	92	92
010100	100	96	94	92
010101	96	98	93	93
010110	98	98	94	93
010111	98	91	92	90
011000	97	92	86	89
011001	96	98	92	91
011010	100	99	95	95
011011	100	99	95	94
011100	99	96	88	88
011101	97	100	90	90
011110	100	97	92	92
011111	100	96	92	92
100000	98	97	95	95
100001	95	98	97	97
100010	100	98	95	95
100011	99	98	98	98
100100	99	96	92	92
100101	93	97	89	90
100110	99	99	94	92
100111	93	97	98	98
101000	100	95	89	90
101001	94	99	85	87
101010	100	98	96	97
101011	99	99	98	99
101100	98	95	97	97
101101	96	99	93	92
101110	98	96	95	96
101111	96	96	97	97
110000	98	91	88	87
110001	95	99	87	89
110010	99	99	92	92
110011	97	99	90	90
110100	99	98	98	98
110101	96	100	96	97
110110	99	100	93	93
110111	99	99	98	98
111000	100	97	92	88
111001	90	98	85	84
111010	100	99	95	93
111011	100	99	100	99
111100	100	94	93	93
111101	94	100	86	86
111110	100	100	95	95
111111	95	95	95	94

Table 21: The average statistical coverage for each exposure scenario, measured in percentage points.

S4: Determinants of Stepwise Selection of Network Features

In this section, we provide an analysis of which features are selected in the stepwise procedure for each simulation scenario. The fraction of simulations in which each adjustment covariate is included depends on each simulation aspect, holding all others constant. Table 22 gives linear regression coefficients evaluating this relationship. Holding all other factors constant, infectious processes in our simulation environment with a high baseline prevalence included more variables than otherwise. Some variables are almost always included ($X^{(1)}$, $X^{(9)}$, and $X^{(11)}$), whereas variables selected less frequently (for example, $X^{(4)} - X^{(8)}$) depend on one or more scenarios, depending on which covariate is considered for inclusion. Finally, the relationship between simulation aspects and covariate inclusion is broadly significant when the associated effect on inclusion exceeds about 0.1, signifying that only strong changes in inclusion by simulation aspect are statistically surprising.

	$X^{(1)}$	$X^{(2)}$	$X^{(3)}$	$X^{(4)}$	$X^{(5)}$	$X^{(6)}$	$X^{(7)}$	$X^{(8)}$	$X^{(9)}$	$X^{(10)}$	$X^{(11)}$	$X^{(12)}$
(Intercept)	1	0.59	0.84	0.22	0.26	0.31	0.49	0.61	0.96	0.92	0.99	0.95
$A = 1$ vs $A = 0$	0	-0.05	-0.11	-0.12	0.04	-0.11	-0.13	0.04	0.02	-0.02	0	-0.08
$\mathbf{a_1}$	0	-0.15	-0.18	0.09	0.29	0.03	-0.14	0.11	0.01	0.16	0	0.16
$\mathbf{a_2}$	0	0.1	0.06	0.14	0.27	0.12	-0.01	0.13	0	-0.03	0	-0.01
$\mathbf{a_3}$	0	-0.04	0.04	0	-0.03	-0.03	-0.02	0	0.01	0.01	0	0.02
$\mathbf{a_4}$	0	-0.03	0.04	-0.06	-0.01	0	0	-0.03	0.01	-0.02	0	0
$\mathbf{a_5}$	0	0.12	-0.34	0.14	-0.05	0.18	0.12	-0.14	-0.03	-0.31	0	-0.28
$\mathbf{a_6}$	0	0.34	0.16	0.01	0.27	0	0.18	0.28	0.03	0.03	0	0

Table 22: The mean difference in the fraction of times each covariate is included in the outcome model under stepwise selection associated with a change in each simulation aspect, holding all other aspects constant. Statistical significance at level $\alpha = 0.05$ is shown as underlined.

$A = 1$ vs $A = 0$	Exposed vs. Unexposed
$\mathbf{a_1}$	High vs. Low Degree
$\mathbf{a_2}$	Powerlaw vs. Poisson
$\mathbf{a_3}$	Assortative vs. Disassortative
$\mathbf{a_4}$	Communities vs. No Communities
$\mathbf{a_5}$	Degree vs. Unit Infectivity
$\mathbf{a_6}$	High vs. Baseline

S5: Estimates of Application Dataset and Outcome Model

In this section, we display the distribution for the degree of all individuals in the Karnataka dataset. In addition, we provide details on the outcome models used in the Application section. Tables 23 and 28 show the covariates used in the outcome models for each adjustment strategy estimating both exposures. Finally, Tables 24-27 and Tables 29-32 Give the estimates, estimated standard deviations, and t- and p-values for statistical significance when adjusting for all other covariates.

Karnataka Degree Distribution

Figure 7 shows While individuals with the largest degree exhibit scale-free behavior, the large majority of individuals exhibit a narrow degree distribution, indicating that a scale-free (powerlaw) degree distribution is not a good fit.

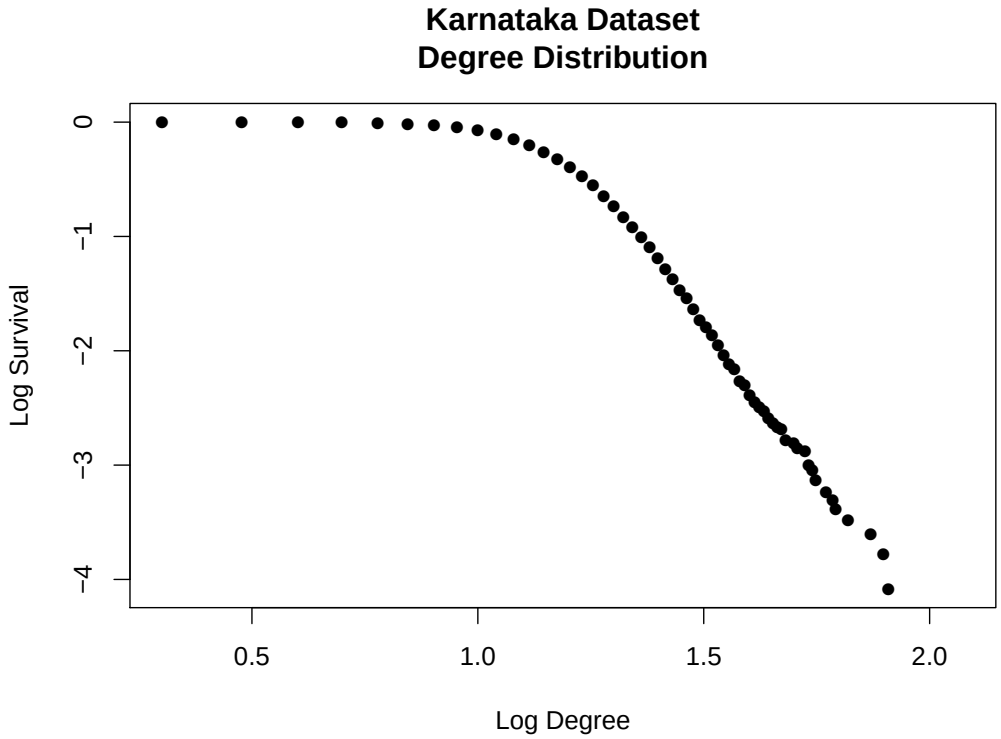

Figure 7: The degree distribution for the Karnataka dataset. The x-axis shows degree, and the y-axis shows the remaining cumulative probability (*survival*) of individuals with at least its corresponding degree. While individuals with the largest degree exhibit scale-free behavior, a large majority of individuals do not, indicating that a Powerlaw degree distribution is not a good fit to the data.

Fraction of Participants Leaders

	Description	Network Covariates Only	Network & Sociodemographic Covariates
θ_2	Sex		Unexposed
θ_3	Age		Exposed;Unexposed
θ_4	Degree	Exposed	Exposed
θ_5	Mean Neighbor Degree	Unexposed	Unexposed
θ_6	Assortativity		
θ_7	LCC Size	Exposed;Unexposed	Exposed;Unexposed
θ_8	Mean Component Size	Exposed;Unexposed	Exposed;Unexposed
θ_9	Total Neighbor Seeds	Unexposed	Unexposed
θ_{10}	Total Cluster Seeds	Exposed	Exposed
θ_{11}	Mins		
θ_{12}	Sums		

Table 23: A table showing the covariates used in the outcome models for each adjustment strategy estimating the effect of the fraction of leaders in each village. In each case, a separate model is used for both exposure groups. The first two strategies use linear logistic regression, whereas the final model employs nonlinear least squares regression.

Augmented GEE (Network Covariates Only)

Exposed

Parameter	Estimate	Standard Error	t-value	p-value
Intercept	0.1936	0.0326	5.9415	0.0000
θ_4	0.0077	0.0014	5.6074	0.0000
θ_7	-0.0006	0.0001	-7.6842	0.0000
θ_8	-0.0005	0.0001	-5.5891	0.0000
θ_{10}	0.0030	0.0004	6.9553	0.0000

Table 24: The estimates, estimated standard deviations, and t- and p-values for statistical significance of each used when adjusting for all other covariates in the exposed network-adjusted augmented GEE model for the exposure of high fraction of leaders.

Unexposed

Parameter	Estimate	Standard Error	t-value	p-value
(Intercept)	0.3951	0.0225	17.5977	0.0000
θ_5	-0.0081	0.0012	-6.8472	0.0000
θ_7	-0.0001	0.0000	-8.3894	0.0000
θ_8	0.0003	0.0001	3.8005	0.0001
θ_9	0.0039	0.0014	2.9035	0.0037

Table 25: The estimates, estimated standard deviations, and t- and p-values for statistical significance of each used when adjusting for all other covariates in the unexposed network- and sociodemographic-adjusted augmented GEE model for the exposure of high fraction of leaders.

Augmented GEE (Network and Sociodemographic Covariates)

Exposed

Parameter	Estimate	Standard Error	t-value	p-value
Intercept	0.2362	0.0385	6.1321	0.0000
θ_3	-0.0013	0.0006	-2.0704	0.0385
θ_4	0.0082	0.0014	5.8544	0.0000
θ_7	-0.0006	0.0001	-7.6616	0.0000
θ_8	-0.0005	0.0001	-5.6084	0.0000
θ_{10}	0.0030	0.0004	6.9282	0.0000

Table 26: The estimates, estimated standard deviations, and t- and p-values for statistical significance of each used when adjusting for all other covariates in the exposed linear and nonlinear covariate adjusted augmented GEE model for the exposure of high fraction of leaders.

Unexposed

Parameter	Estimate	Standard Error	t-value	p-value
Intercept	0.4344	0.0249	17.4641	0.0000
θ_2	0.0162	0.0085	1.9094	0.0562
θ_3	-0.0013	0.0003	-3.8254	0.0001
θ_5	-0.0078	0.0012	-6.4798	0.0000
θ_7	-0.0001	0.0000	-8.4663	0.0000
θ_8	0.0003	0.0001	3.7191	0.0002
θ_9	0.0039	0.0014	2.8641	0.0042

Table 27: The estimates, estimated standard deviations, and t- and p-values for statistical significance of each used when adjusting for all other covariates in the unexposed network-adjusted augmented GEE model for the exposure of high fraction of leaders.

Fraction of Participants Using Self-Help

	Description	Network Covariates Only	Network & Sociodemographic Covariates
θ_2	Sex		Unexposed
θ_3	Age		Unexposed
θ_4	Degree	Exposed	Exposed
θ_5	Mean Neighbor Degree	Exposed;Unexposed	Exposed;Unexposed
θ_6	Assortativity	Exposed	Exposed
θ_7	LCC Size	Exposed;Unexposed	Exposed;Unexposed
θ_8	Mean Component Size	Exposed;Unexposed	Exposed;Unexposed
θ_9	Total Neighbor Seeds	Unexposed	Unexposed
θ_{10}	Total Cluster Seeds		
θ_{11}	Mins		
θ_{12}	Sums	Exposed	Exposed

Table 28: A table showing the covariates used in the outcome models for each adjustment strategy estimating the effect of the fraction of individuals concurrently participating in the self-help program. In each case, a seperate model is used for both exposure groups.

Augmented GEE (Network Covariates Only)

Exposed

Parameter	Estimate	Standard Error	t-value	p-value
Intercept	0.0452	0.0530	0.8526	0.3939
θ_4	0.0073	0.0015	4.9436	0.0000
θ_5	0.0046	0.0028	1.6352	0.1021
θ_6	0.8152	0.1031	7.9059	0.0000
θ_7	-0.0001	0.0000	-1.5470	0.1220
θ_8	-0.0003	0.0001	-3.8145	0.0001
θ_{12}	-0.0034	0.0008	-4.1704	0.0000

Table 29: The estimates, estimated standard deviations, and t- and p-values for statistical significance of each used when adjusting for all other covariates in the exposed linear and nonlinear covariate adjusted augmented GEE model for the exposure of high fraction of self-help uptake.

Unexposed

Parameter	Estimate	Standard Error	t-value	p-value
Intercept	0.3585	0.0224	16.0091	0.0000
θ_5	-0.0077	0.0012	-6.3968	0.0000
θ_7	-0.0001	0.0000	-7.8174	0.0000
θ_8	0.0004	0.0001	4.6739	0.0000
θ_9	0.0042	0.0013	3.2387	0.0012

Table 30: The estimates, estimated standard deviations, and t- and p-values for statistical significance of each used when adjusting for all other covariates in the unexposed network-adjusted augmented GEE model for the exposure of high fraction of self-help uptake.

Augmented GEE (Network and Sociodemographic Covariates)

Exposed

Parameter	Estimate	Standard Error	t-value	p-value
Intercept	0.0452	0.0530	0.8526	0.3939
θ_4	0.0073	0.0015	4.9436	0.0000
θ_5	0.0046	0.0028	1.6352	0.1021
θ_6	0.8152	0.1031	7.9059	0.0000
θ_7	-0.0001	0.0000	-1.5470	0.1220
θ_8	-0.0003	0.0001	-3.8145	0.0001
θ_{12}	-0.0034	0.0008	-4.1704	0.0000

Table 31: The estimates, estimated standard deviations, and t- and p-values for statistical significance of each used when adjusting for all other covariates in the exposed network-adjusted augmented GEE model for the exposure of high fraction of self-help uptake.

Unexposed

Parameter	Estimate	Standard Error	t-value	p-value
Intercept	0.4030	0.0247	16.3435	0.0000
θ_2	0.0178	0.0085	2.1068	0.0352
θ_3	-0.0015	0.0003	-4.4782	0.0000
θ_5	-0.0073	0.0012	-5.9668	0.0000
θ_7	-0.0001	0.0000	-7.8681	0.0000
θ_8	0.0004	0.0001	4.6036	0.0000
θ_9	0.0042	0.0013	3.1995	0.0014

Table 32: The estimates, estimated standard deviations, and t- and p-values for statistical significance of each used when adjusting for all other covariates in the unexposed network-adjusted augmented GEE model for the exposure of high fraction of self-help uptake.

References

[1] Brian Karrer and Mark EJ Newman. Stochastic blockmodels and community structure in networks. *Physical Review E*, 83(1):016107, 2011.